Primordial Germ Cell Development in the Poeciliid, *Gambusia holbrooki*, Reveals Shared Features Between Lecithotrophs and Matrotrophs

Komeil Razmi* and Jawahar G. Patil*

Laboratory of Molecular Biology, Fisheries and Aquaculture Centre, Institute for Marine and Antarctic Studies, University of Tasmania, Taroona, TAS, Australia

Metazoans exhibit two modes of primordial germ cell (PGC) specification that are interspersed across taxa. However, the evolutionary link between the two modes and the reproductive strategies of lecithotrophy and matrotrophy is poorly understood. As a first step to understand this, the spatio-temporal expression of teleostean germ plasm markers was investigated in *Gambusia holbrooki*, a poecilid with shared lecitho- and matrotrophy. A group of germ plasm components was detected in the ovum suggesting maternal inheritance mode of PGC specification. However, the strictly zygotic activation of *dnd-β* and *nanos1* occurred relatively early, reminiscent of models with induction mode (*e.g.,* mice). The PGC clustering, migration and colonisation patterns of *G. holbrooki* resembled those of zebrafish, medaka and mice at blastula, gastrula and somitogenesis, respectively—recapitulating features of advancing evolutionary nodes with progressive developmental stages. Moreover, the expression domains of PGC markers in *G. holbrooki* were either specific to teleost (*vasa* expression in developing PGCs), murine models (*dnd* spliced variants) or shared between the two taxa (germline and somatic expression of *piwi* and *nanos1*). Collectively, the results suggest that the reproductive developmental adaptations may reflect a transition from lecithotrophy to matrotrophy.

Keywords: germline development, germ plasm, invasive species, evolutionary adaptation, viviparity

INTRODUCTION

Primordial germ cells are the stem cells of life; they give rise to gametes, safeguarding the reproductive function of an individual and transfer its genetic material to ensuing generations. Two patterns of germ cell development are known in sexually reproducing animals; 1) Induction mode, where epigenetic reprogramming in a group of pluripotent cells induces PGC identity (Wang and Cao, 2016) and 2) Preformation mode, in which pre-packaged molecules in gametes, *i.e.,* germ plasm components, trigger PGC specification in early zygotes (Raz, 2002; Santos and Lehmann, 2004) which determine their germline fate and protect their identity against surrounding soma. Despite earlier thoughts, the germ plasm acquisition is not confined to primitive animals, but repeatedly shared in higher taxa (Ewen-Campen et al., 2010; Whittle and Extavour, 2017) particularly in those that exhibit lecithotrophy. With high species diversity, fish taxa have evolved both modes of PGC specification (Walvig, 1963; Extavour and Akam, 2003; Hansen and Pelegri, 2021). With majority of oviparous teleost including research models (Raz, 2002; Herpin et al., 2007) and commercial species (Nagasawa et al., 2013; Su et al., 2014) following the preformation

mode, while most chondrichthyans (*i.e.,* cartilaginous fishes) following induction mode (Extavour and Akam, 2003) that also typically exhibit a degree of matrotrophy. However, little is known in poeciliids, which interestingly share aspects of both lecitho- and matrotrophy such as in the *G. holbrooki* (Mousavi and Patil, 2021).

Typically, PGCs undergo several developmental stages before transforming into functional germ cells. These begin with PGC specification regulated by parental derivates (Hong et al., 2016; Zhu et al., 2018) or epigenetic reprogramming (Yabuta et al., 2006; Saitou and Yamaji, 2012), followed by mobility acquisition to reach gonad anlage (Richardson and Lehmann, 2010; Paksa and Raz, 2015), and eventually attaining sexual identity, influenced by genetic/intrinsic (Devlin and Nagahama, 2002; Matsuda, 2005) or environmental/extrinsic (Baroiller et al., 2009) cues. Cumulative evidence suggests that each of these stages are governed by a group of molecules which recruit epigenetic machinery (Andersen et al., 2012), RNA interference apparatus (Giraldez et al., 2006) and/or signaling pathways (Boldajipour et al., 2008) safeguarding PGCs from somatic differentiation (Gross-Thebing et al., 2017), ectopic migration and apoptosis (Lai et al., 2012). Despite shared biochemical pathways, fundamental differences in the mode of PGC specification (*i.e.,* preformation vs induction) exists, as is obvious from spatio-temporal expression profiles of these molecules between taxa (Evans et al., 2014; Crother et al., 2016). For instance, during zebrafish (*Danio rerio*) embryogenesis, the maternally supplied *vasa* (Hartung et al., 2014) and *nanos1* (Koprunner et al., 2001) maintain the specificity and quantity of PGCs, respectively. Similarly, *dead end* (*dnd*), a regulator of the RNA interference machinery, is well conserved in teleost, whose maternal transcripts mark PGC sequestration and migration (Ketting, 2007) in models such as zebrafish (Weidinger et al., 2003), medaka (Hong et al., 2016) and Atlantic salmon (Nagasawa et al., 2013). However, in higher vertebrates with induction mode—*e.g.,* axolotl (Chatfield et al., 2014) and mouse (Saitou and Yamaji, 2010)—germ plasm does not form and the maternal deposit is erased in early stages of embryonic development (*i.e.,* cleavage). Instead, epigenetic machinery triggers PGC specification via bone-morphogenetic (BMP) signaling (Saitou et al., 2012; Seisenberger et al., 2012; Donoughe et al., 2014). Also, unlike medaka (Hong et al., 2016) and *Xenopus* (Taguchi et al., 2014), *Dnd* mutation (Sakurai et al., 1995; Youngren et al., 2005) and *Nanos1* ablation (Haraguchi et al., 2003) in mice do not affect PGC specification and fertility respectively. Therefore, despite the conserved regulatory pathways and set of molecules, PGC specification shows a shift in their developmental pattern in lecithotrophs with no maternal care (*e.g.,* zebrafish) and low maternal care, *e.g.,* medaka, (Morrison et al., 2017; Murata et al., 2020), to those distinct to matrotrophs (*e.g.,* mouse). Hence models such as poeciliids, *e.g.,* gambusia, with shared lecithotrophy (*i.e.,* where embryos receive nutrients only through the yolk) and matrotrophy (*i.e.,* where embryos receive nutrients from the mother) are likely to advance our current understanding as to how germline specification and maintenance evolve and function.

The ovo-viviparity of poeciliids is accompanied with interesting and complex alteration in their biology of reproduction including developing spermatozoa bundles (Grier et al., 1981) and an intromittent organ *i.e.,* gonopodia for deposition of sperm (Gasparini et al., 2011) in males, and matrotrophy, intrafollicular gestation (Pollux et al., 2014; Roberts et al., 2016) and superfetation (Norazmi-Lokman et al., 2016; Guzman-Barcenas and Uribe, 2019) in females. Moreover, the pseudo-placenta which evolved in poeciliids provides a maternal-fetal interface (Olivera-Tlahuel et al., 2018) sharing reproductive traits with placentalia. However, the consequences of this evolutionary convergence on germ cell formation and gonadogenesis is poorly understood.

In this regard, *G. holbrooki* presents as a particularly attractive poeciliid on count of its now wide global distribution (Norazmi-Lokman et al., 2021), short reproductive cycle (Norazmi-Lokman et al., 2016), well-documented embryology (Mousavi and Patil, 2021), close evolutionary relatedness to higher vertebrates (Furness et al., 2019; Furness et al., 2021) and notoriety as a pest fish (Ayres et al., 2012; Patil, 2012). A number of approaches to control its pest populations have been ineffective, particularly at large spatial scales. Hence, gaining insight into cellular and genetic pathways of germ cell development and gonadogenesis is expected to enhance our understanding of its reproductive biology to facilitate genetic control (Patil, 2012), whilst providing insights into comparative mechanisms of PGC development. This study for the first time examined PGC development across a range of embryonic stages of *G. holbrooki*, discerning shared features with other teleost and higher vertebrates, highlighting its utility to decipher comparative mechanisms of reproduction as well as direct application to control pest populations.

METHODS

Wild Fish Collection and Housing
The fish were collected from the Tamar Island Wetland Reserve, Tasmania (41°23.1′S; 147°4.4′E) and reared in a dedicated small fish facility at Institute for Marine and Antarctic Studies (IMAS), Taroona, University of Tasmania. The rearing conditions are summarized in the **Supplementary Table S1**. The fish were fed with commercial pellets (TetraMin1 tropical granules, Germany) and freshly hatched Artemia nauplii (INVE Aquaculture, United States). The experimental ova and developing embryos were obtained from gravid females (Norazmi-Lokman et al., 2016) and staged (Mousavi and Patil, 2021) as previously described. All experimental procedures were approved by the University of Tasmania Animal Ethics Committee (Permit No. A12787).

RNA Isolation and qRT-PCR
To evaluate the expression profile of key PGC markers during early development, total RNA from seven distinct developmental stages (Mousavi and Patil, 2021) including ovum (*i.e.,* vitellogenic oocytes stage V obtained from virgin females), cleavage (*i.e.,* mid-morula stage) blastula (*i.e.,* 1000-cell stage), gastrula (*i.e.,* the

onset of embryonic shield elongation), early segmentation, late segmentation, and early pharyngula were isolated and used in quantitative PCR assay (n = 4-8 embryos/sex/developmental stage). To distinguish the spatial domains (*i.e.,* anterior and/or posterior of the developing embryos) of expression using end-point PCR, somite stage embryos (n = 5) were used. For this, most of the yolk was removed by puncture using Dumont #5 fine forceps (F.S.T, Canada) and the tissue was partitioned as head (anterior to otic vesicle) and trunk halves (**Figure 2C**) using a fine straight tipped dissecting knife (10,055-12, F.S.T, Canada), with each half processed separately for RNA isolation. The expression of the target genes in adult liver, kidney, spleen, skeleton muscle, heart, eyes, brain, testis and ovary (n = 4 sex/tissue) were also tested.

Individual embryos and adult tissues were rinsed in cold PBS, infiltrated with RNAlater (Sigma-Aldrich, Missouri, United States) and stored at -80°C until nucleic acid extraction. The RNA and DNA from individual embryos and 15–25 mg of tissues were isolated using AllPrep DNA/RNA Mini Kit (QIAGEN, United States). The residual genomic DNA in RNA extracts was removed using Ambion™ DNase (Thermo Scientific, United States) and RNA was purified by Monarch® RNA Clean-up Kit (New England Biolabs). The quantity of isolated RNA was measured by Qubit® four Fluorometer (ThermoFisher Scientific, Massachusetts, United States) and the RNA integrity was confirmed visually using agarose gel electrophoresis. The purified RNA was then reverse transcribed using MMLV Reverse Transcriptase (Takara, Kusatsu, Japan), with a final concentration of 6–230 and 250 ng/μl for embryos and tissues, respectively. The synthesised cDNA from adult tissues and somite embryos were later used in end-point PCR assays.

cDNA Cloning and Full-Length Sequencing

To obtain full length cDNA of the genes from *G. holbrooki*, the predicted cDNA sequences from different poeciliid species were extracted from the NCBI database and multiple sequence alignments were applied using MUSCLE (Edgar, 2004). Subsequently, degenerate primers were designed based on highly conserved regions of the target cDNA homologues using Geneious Prime® (version 2020.2.3). The primers were recruited to amplify target cDNA fragments through end-point PCR, the products were purified, cloned into pCR®2.1-TOPO® vectors using TOPO™ TA Cloning Kit (Life Technologies Corporation, CA, United States) and sequenced. The resulting sequences were used to design *G. holbrooki* specific primers that were used in Rapid Amplification of cDNA Ends (RACE) PCR to obtain full-length cDNA using GeneRacer™ Kit (Life Technologies) according to the manufacturer's protocol.

Design of qPCR Primers and Data Normalisation

The qPCR assay primers (**Supplementary Table S2**) were designed using Geneious Prime® (2020.2.3) with care to avoid self-dimer and secondary structures (Untergasser et al., 2012). Their efficiency was also tested at different dilutions for each

gene, separately. The real time PCR mix (10 μl) comprised of 1X iTaq Universal SYBR Green Supermix (Bio-Rad, NSW, Australia), 5–10 ng cDNA Template, 0.4 μM of each primer, and adjusted to 10 μl using MilliQ water. Duplicate reactions were run for each cDNA sample using CFX96 Touch Real-Time PCR Detection System (Bio-Rad, NSW, Australia). Melting curve analysis, gel visualisation and sequencing of qPCR products were subsequently performed to check unwanted products and gDNA contamination.

Four housekeeping genes, namely *rps18*, *gapdh*, *pgk1* (Panina et al., 2018), and *β-actin* (Kwan and Patil, 2019) were tested for biological normalisation of qPCR data through geometric averaging of the candidate genes using geNorm algorithm (Vandesompele et al., 2002; Hellemans et al., 2007) in qbase + software (version 3.0, Biogazelle, Belgium). The *β-actin* with no sex-biased expression was selected to normalise qPCR data as the most stable housekeeping gene (M value 0.41). The relative transcription of target genes was calculated using the comparative threshold cycle (Cq) method with efficiency correction (Ruijter et al., 2009). Relative expression of genes of interest (ΔCq) was calculated against the selected reference gene and presented in plots. The expression fold changes presented were computed using the $2^{(-\Delta\Delta Cq)}$ method (Livak and Schmittgen, 2001).

Statistical Analysis

The qPCR data was subject to analysis of variance (ANOVA) to identify significant differences between experimental groups. When applicable, Tukey HSD test used to compare the significance level of differences treatments. Normality of the data was tested with the Shapiro-Wilk test. The significance was set at $p < 0.05$.

Whole Mount *in situ* Hybridization

The WM-ISH was used to investigate the spatial expression of target genes in several embryonic stages (*i.e.,* from late cleavage to early pharyngula). To ensure specificity, the sense and antisense RNA probes were generated from a less conserved domains such as untranslated regions (Thisse and Thisse, 2008). The respective cDNAs were first inserted into pCR®2.1-TOPO vector. DIG-labelled RNA probes were produced by *in vitro* transcription using T7/T3 RNA polymerase (NEB) and DIG RNA labelling mix (Roche, Mannheim, Germany). Any traces of cDNA in the probe were eliminated using Ambion™ DNase (Thermo Scientific, United States), purified by ethanol precipitation and stored with RNase inhibitor, RNasein® Plus (Promega, United States) at -20°C.

The WM-ISH followed those described for small fish embryos (Thisse and Thisse, 2008) with modifications. Briefly, the dissected clutches of developing embryos were individually detached from placenta, rinsed with cold PBS, and fixed using 4% paraformaldehyde (Emgrid) overnight at 4°C. The fixed embryos were washed in PBS containing 0.1% Tween 20 (PBT), progressively dehydrated with PBT-methanol, and stored in 100% methanol until use. The embryos at early and mid-pharyngula stages were depigmented before dehydration using 3% H_2O_2 and 1% KOH. On the day of hybridization,

the embryos were sequentially rehydrated in four stages with progressively increasing concentrations of methanol-PBT, manually dechorionated, permeabilized with 10–25 µg/ml proteinase K (Bioline) and postfixed with 4% paraformaldehyde for 30 min. The embryos were prehybridized at 68°C for 3 h in hybridization buffer (50% formamide, 5X SSC, 0.01% Tween 20, Torula Yeast tRNA, 50 µg/ml heparin) and hybridized in fresh buffer containing antisense RNA probes (100–250 ng/ml) at 67–69°C for 16–24 h, as required for target gene and developmental stage. This was followed by stringency washes in PBST, with progressively lower salt concentrations, to remove any non-specifically bound probes. For immuno-labelling, non-specific binding was first prevented using blocking solution (5% blocking reagent (Roche) in maleic acid buffer containing 0.1% Tween 20). The embryos were then treated with 1:3,000–1:5,000 anti-DIG alkaline phosphatase (AP) antibody (Roche) at 4°C for 16 h. The antibody-labelled embryos were washed with PBT 8 times, 30 min each, at room temperature, under gentle agitation. For staining, the embryos were first treated with staining buffer (100 mM Tris HCl pH 9.5, 50 mM MgCl2, 100 mM NaCl, 0.1% Tween 20) three times by replacing with fresh buffer every 10 min and then incubated in BM-purple stain (Roche) at room temperature and protected from light. The optimum staining time was adjusted according to developmental stages and target genes ranging from 5 to 35 h. Following staining, the embryos were washed in PBT until all excess stain was removed and postfixed with 4% paraformaldehyde overnight at 4°C. The fixed embryos were washed and stored in PBS for imaging using MZ16FA stereomicroscope (Leica Microsystems, Germany).

Genetic Sexing of Embryos

The isolated DNA (co-extracted with RNA using AllPrep DNA/RNA Mini Kit) were used for genetic testing as previously described for this species (Kwan and Patil, 2019; Patil et al., 2020). Briefly, PCR mix (10 µl) comprised of 1X MyTaq™ HS Red mix (Meridian Life Science, OH, United States), 0.4 µM of each primer and 50 ng of genomic DNA template. Thermal cycling (T100™ Thermal Cycler, Bio-Rad Laboratories, NSW, Australia) consisted of 95°C for 1 min, followed by 30 cycles of 95°C for 5 s, 60°C for 5 s, and 72°C for 20 s. Female and male specific amplicons were visualised using gel electrophoresis.

RESULTS

The Pattern of PGC Migration in *G. holbrooki*

The *vasa* mRNA signals were first detectable in late cleavage stages, emerging as a few tiny spots distributed throughout the blastomere (**Figure 1A**). At this stage, the signals were partially obscured by egg yolk (*i.e.,* meroblastic cleavage) and buried deep in the cells mass, partially masked by glare of the large oil-droplets beneath. At early blastula (1000-cell stage), concurrent with increased blastoderm area (400–450 µm) and asynchronous cell divisions, the *vasa* signal was intense at three distinct spots that were asymmetrically distributed with one larger and

darker than the other two (**Figure 1B**). At mid-blastula, four distinctive spots were detectable buried underneath the layer of cells at almost the same geometrical plane (**Figure 1C**). At late blastula, the *vasa*-positive signals had numerically increased and arranged peripherally to the blastodisc in four clusters (**Figure 1D**).

At the onset of the gastrula stage (*i.e.,* corresponding to 50%-epiboly in zebrafish and egg cylinder in mice), the blastoderm had begun to expand within a crater-like depression over the surface of the yolk at the animal pole. Here, the *dnd-α* signals had coalesced and appeared as two compact clusters of cells located at the margin of the dome (**Figure 1E**) where both the dome and the yolk boundaries were difficult to distinguish and so were the anterior-posterior axis (**Figure 1E**). For the first time, from mid to late gastrula, the anterior-posterior axis of the embryo was distinguishable and the optic primordia began to form as the body-axis lengthened and thickened. Here, the *vasa*-positive cells appeared pellucid and were located at the posterior half of the embryo. At this stage, the PGCs were clustered at the junction of developing embryo and the yolk, close to posterior of the trunk, however, the individual germ cell precursors were distinguishable (**Figure 1F**).

At the onset of somitogenesis, concurrent with considerable expansion of the head, rudimentary brain formation and first visible somites, the two clusters of PGCs were still visible, one on either side of the body axis, forming narrow queue of cells (**Figures 1G, 4D**). Based on the spatial distribution of PGCs two directions of motility were discernible, with the two clusters beginning to 1) converge inwards, *i.e.,* PGC clusters moved towards each other and 2) migrating anteriorly.

As evident from migrating signals at early to mid-somitogenesis, coinciding with significant body elongation, PGCs exhibited a relatively enhanced mobilisation compared to late gastrula stage. Specifically, at 12–14 somite stage, where solid optic capsule and otic vesicles were also visible, the two PGC clusters were clearly observed extending from the sixth to eighth somite (**Figure 1G**). The PGC clusters maintained their integrity (*i.e.,* cells moving in a close vicinity to each other), however, the narrow queue of cells progressively clustered tightly (thickened and shortened cluster of cells), compared to preceding developmental stage. At late segmentation, PGC clusters were observed on either side of the body axis, directly underneath the somites and the spinal cord, in closest vicinity to each other (**Figure 1H**). At early pharyngula, the PGCs had migrated and coalesced at the genital ridge and remained in two distinctive clusters (**Figure 3E**).

Spatio-Temporal Expression of PGC Markers in *G. holbrooki*

Of all the PGC markers, only *dnd* had the two spliced variants; the longer variant, *dnd-α*, contained five exons with 1,122 bp CDS, while the shorter *dnd-β* (1,056 bp CDS) contained six exons. Based on end-point PCR, all the candidate PGC markers were expressed in adult ovary and testis, with additional expression of *nanos1* in brain
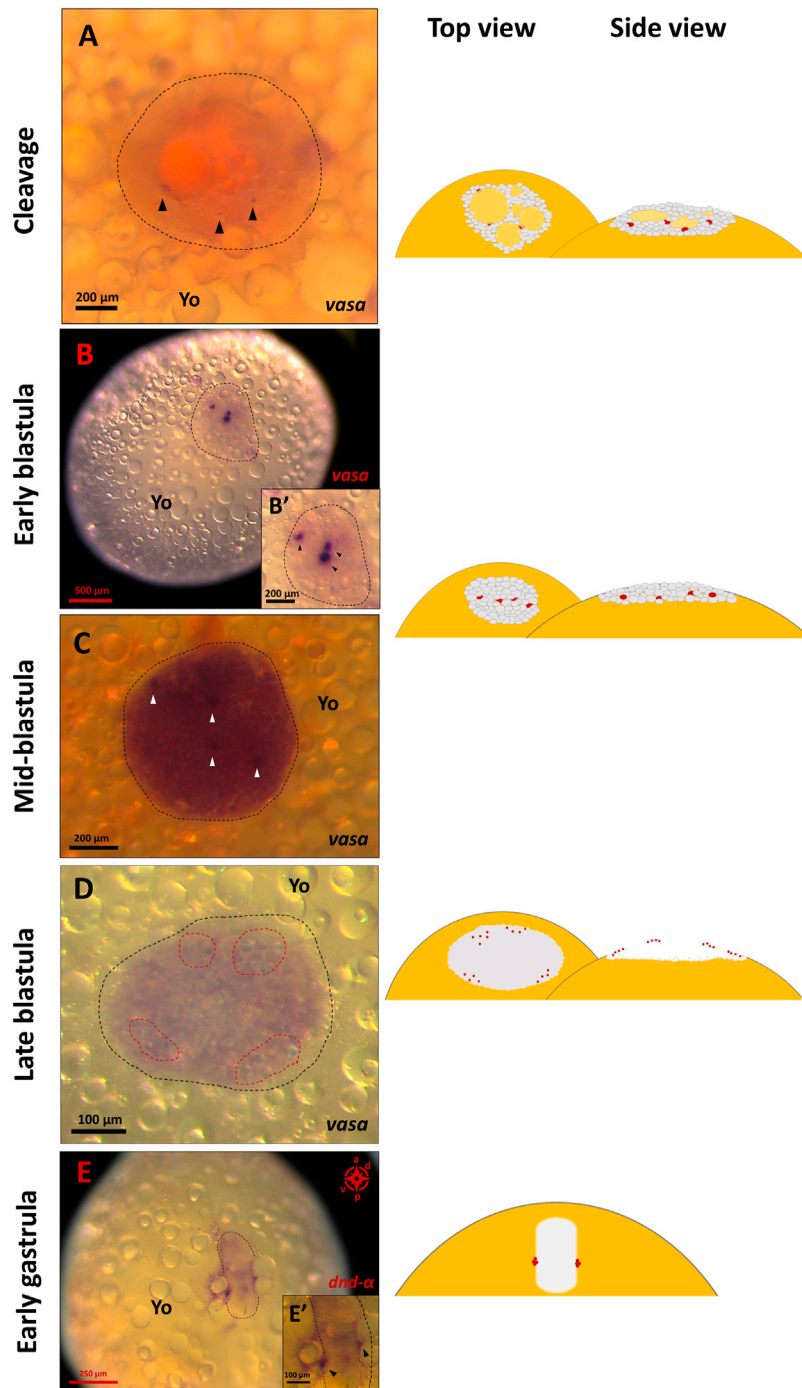
FIGURE 1 | PGC formation and migration in *G. holbrooki*. WISH panels showing the actual and schematic locations of PGC during *G. holbrooki* embryogenesis. The PGC markers, *vasa* or *dnd-α* signals at nine developmental stages are presented. The *vasa*-positive cells are first detectable ((A), black arrowhead) emerging as a few tiny spots distributed throughout the cell mass (n = 3). At early blastula (B), the *vasa* signal was intensified in a few distinctive regions (black arrowhead in close-up B′) with asymmetric distribution (n = 4). Later, four distinctive spots ((C), white arrowhead) are detectable buried underneath the superficial layer of cells (n = 3). At late blastula (D), the *vasa*-positive signals increase and appear peripherally as small clusters (n = 4). At early gastrula (E), the PGCs coalesce as two compact clusters of cells (black arrowhead in the close-up E′) located at the margin of the dome (n = 4). At late gastrula (F), the PGCs were located at the posterior half of the embryo (n = 3). During segmentation stages ((G), n = 5 and (H), n = 4), the PGC clusters migrate convergently and anteriorly, and at early pharyngula (I), they eventually home at genital ridge (red arrowheads) and form a bi-lobular presumptive gonad (n = 7). The black dashed lines indicate the area of the cleavage plane and blastodisc (A,B), and embryonic axis (E,F,G,H,I) respectively. The red dashed lines (D) show the signals clustered in four groups. The red dots in schematics represent relative position of the PGC marker signals. Op, optic bud; Yo, yolk; Seg, segments.
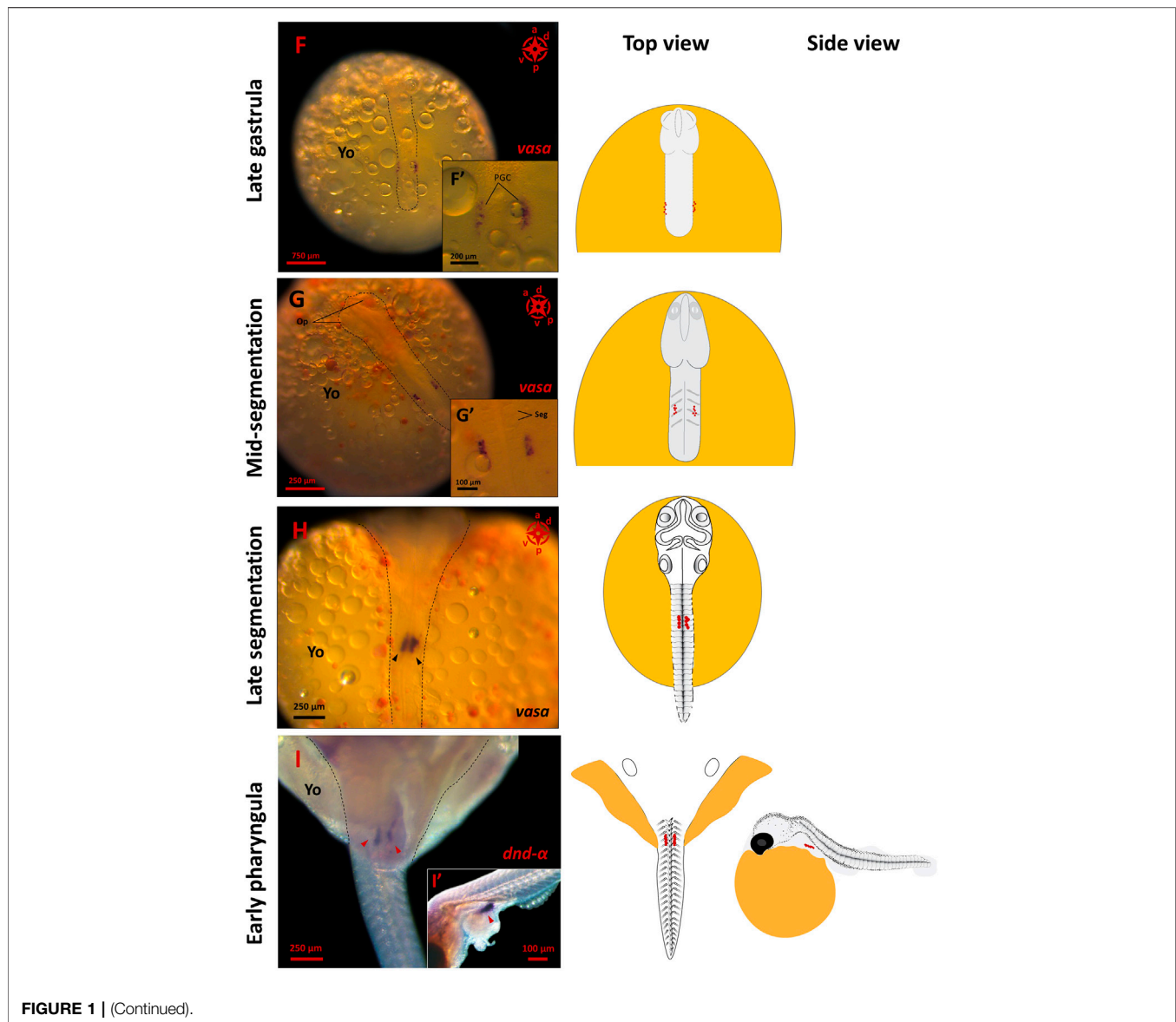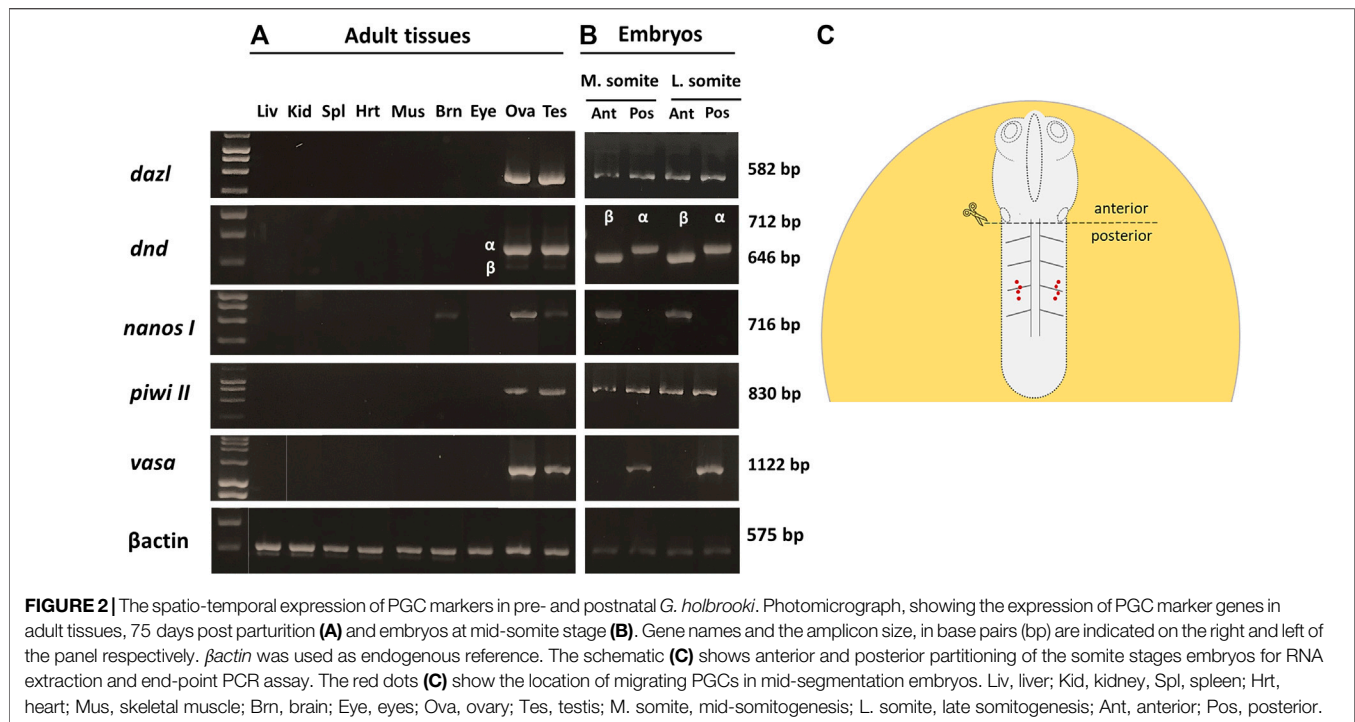
FIGURE 1 | (Continued).

(**Figure 2A**). As for the embryonic expression, two of which were detected in the posterior (*vasa* and *dnd-α*) and anterior (*nanos1* and *dnd-β*) halves of somitogenesis embryos, while *piwiII* and *dazl* were detected in both consistent with WMISH observation (**Figures 2B,C**). More specifically, *vasa* (**Figure 1**), *dnd-α* (**Figures 3A,C,D**), *dazl* (**Figure 4B**) and *piwiII* (**Figure 4D**) transcripts expressed in the posterior half overlapped with the location of nascent PGCs. While the anterior expression of *dazl* was found as strong signal in the otic vesicles with a weak signal in the eyes (**Figure 4A**). The anterior expression of *piwiII* corresponded to large part of the developing brain but restricted to mesencephalon and diencephalon (**Figure 4C**). The *dnd-β* was first detected at the anterior region at early gastrula (**Figure 3B**), then expanded on both sides of the developing brain at early segmentation (**Figure 3D**) and cerebellum during early pharyngula (**Figure 3F**).

Quantitatively, four of these PGC markers (*dnd-α*, *dazl*, *piwi II*, and *vasa*) were detected in unfertilised egg (**Figure 5**), with *nanos1* and *dnd-β* barely detectable or absent (**Figure 6** and **Table 1**). The maternally expressed genes showed a comparable trend in cleavage and blastula (**Table 1**). However, the maternally silent genes were strongly upregulated ($p < 0.05$, **Table 1**) at early embryogenesis (*i.e.,* cleavage). Comparing the quantitative expression of maternally inherited genes between stages (**Table 1**), a significantly transient surge was observed at gastrula stage ($p < 0.05$) with a female-biased trend ($p < 0.05$).

DISCUSSION

While a previous study (Pala, 1970) investigated PGCs in *G. holbrooki*, this was limited to late developmental stages and gross

FIGURE 2 | The spatio-temporal expression of PGC markers in pre- and postnatal *G. holbrooki*. Photomicrograph, showing the expression of PGC marker genes in adult tissues, 75 days post parturition **(A)** and embryos at mid-somite stage **(B)**. Gene names and the amplicon size, in base pairs (bp) are indicated on the right and left of the panel respectively. *βactin* was used as endogenous reference. The schematic **(C)** shows anterior and posterior partitioning of the somite stages embryos for RNA extraction and end-point PCR assay. The red dots **(C)** show the location of migrating PGCs in mid-segmentation embryos. Liv, liver; Kid, kidney, Spl, spleen; Hrt, heart; Mus, skeletal muscle; Brn, brain; Eye, eyes; Ova, ovary; Tes, testis; M. somite, mid-somitogenesis; L. somite, late somitogenesis; Ant, anterior; Pos, posterior.

cell morphology. In contrast, a detailed PGC developmental dynamics presented here captures shared evolutionary features of both lecitho- and matrotrophic vertebrates.

Evidence for Maternal Inheritance of PGC Specification

The relatively high expression of PGC markers tested (*dazl*, *dnd-α*, *piwi II*, and *vasa* but not *nanos1*) in unfertilised eggs of *G. holbrooki* implies their maternal inheritance and suggests PGC specification is determined by preformation mode. This pattern is similar to those observed in oviparous species such as zebrafish (Kaufman and Marlow, 2016) and medaka (Herpin et al., 2007) as well as those of *Drosophila* (Rongo and Lehmann, 1996), and *Xenopus* (Chan et al., 2007). However, in mice, mechanical ablation of vegetal or animal pole of the fertilised egg did not arrest the development of viable and fertile offspring (Zernicka-Goetz, 1998). This was later confirmed by the evidence that nuage was not detectable in unfertilised and fertilised murine eggs (Toyooka et al., 2000) suggesting PGC specification is governed by zygotic determinants in mice.

In teleosts, the maternal factors such as *tdrd6* safeguards proper germ plasm segregation (Roovers et al., 2018), while, *dnd* (Hong et al., 2016; Zhu et al., 2018) and *dazl* (Li et al., 2016) are necessary for maintaining PGC identity, with *nanos1* (Koprunner et al., 2001), and *vasa* (Braat et al., 2001; Li et al., 2009) providing signals for their proliferation and correct migration. The maternal accumulation of these markers in ova supports early germline sequestration in *G. holbrooki* with comparable functions reported for other fish models.

Relatively Early Onset of Zygotic Activation Mimics Those of Mouse

The presence of *nanos1* and *dnd-β* transcripts in post-fertilisation embryos, but not in ova suggests its zygotic origin. Their first appearance at mid-cleavage is a preliminary evidence of zygotic genome activation (ZGA) onset which is earlier compared to what occurs at mid-blastula in zebrafish (Jukam et al., 2017). By inference, this appears a relatively early model of global zygotic activation among teleosts. The timing of MZT is not conserved across species nor follows a pattern of evolutionary hierarchy. For example, the earliest ZGA has been reported in sea urchin (Tu et al., 2014) and mice (Abe et al., 2015) at first cell division, while in zebrafish (Pelegri, 2003; Lindeman and Pelegri, 2010; Aanes et al., 2011) and *Drosophila* (Atallah and Lott, 2018), its activation is postponed until the 10th and eighth cycles, respectively. Typically, the onset of global ZGA are evaluated by an array of cellular events. For example, cell cycle intervals lengthen, as zygotic transcription interrupts DNA replication (Rothe et al., 1992), coinciding with the initiation of ZGA. However, in species with relatively early ZGA (e.g., mice and *G. holbrooki*), demarcation of ZGA with longer cell cycle intervals are less likely to be useful. Instead, more refined indicators such as the appearance of maternal transcript repressors (Ruzov et al., 2004), increased chromatin accessibility (Liu et al., 2018) and dilution of histone concentration (Joseph et al., 2017) may provide greater precision.

Epigenetic Trigger May Explain PGC Markers Surge

Activation of PGC markers (*dazl*, *piwi II*, and *dnd-α*) at gastrula in *G. holbrooki* is similar to those in mice (Smith and Meissner, 2013) and zebrafish (Potok et al., 2013), known to be initiated via epigenetic
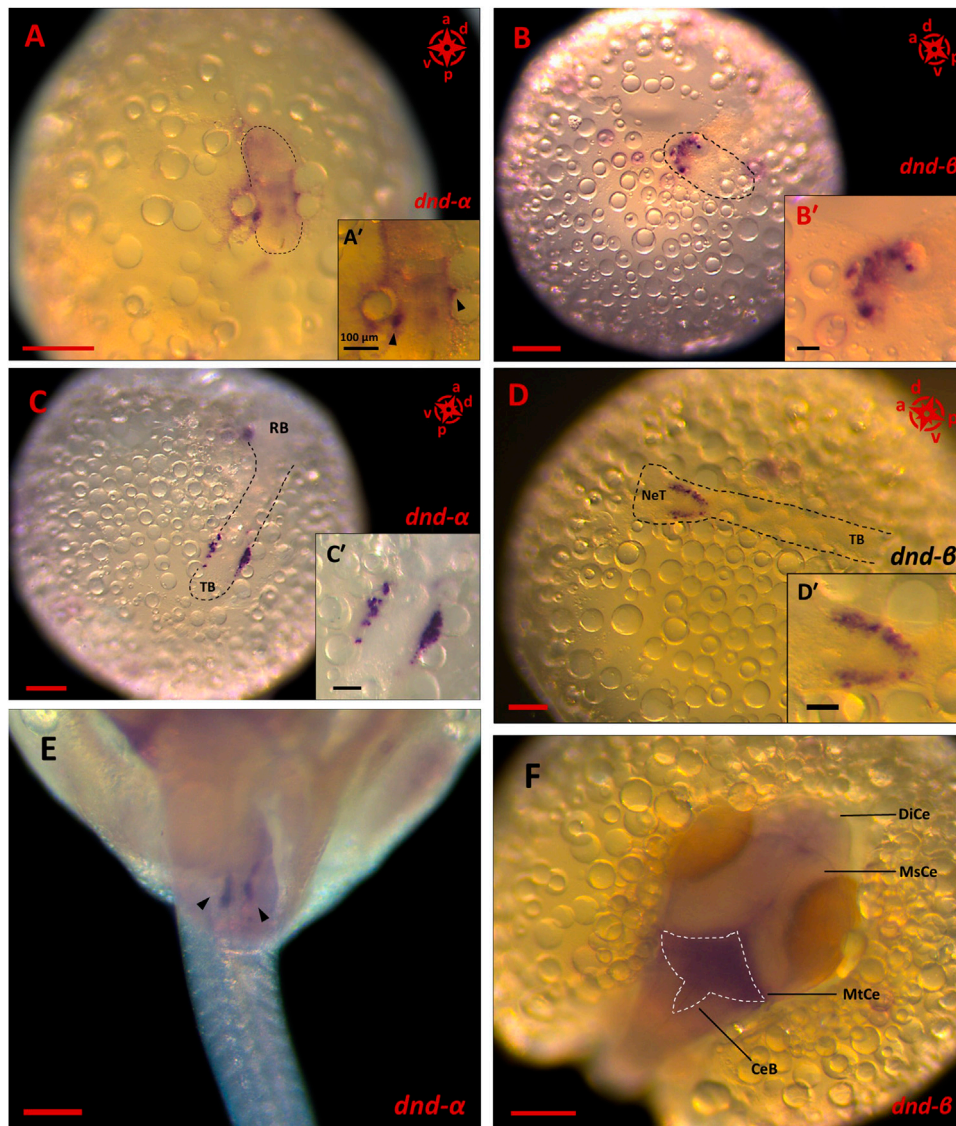
FIGURE 3 | The expression pattern of *dnd* spliced variants in embryonic stages of *G. holbrooki*. WISH panels showing spatial expression of *dnd* spliced variants at three developmental stages of *G. holbrooki*. *dnd-α* is expressed in the posterior region of early gastrula (**(A)**, and close up inset, n = 4), with condensed signals at two spots (black arrowheads in A′) in the peripheral embryonic shield. At early segmentation (n = 4), two clusters of *dnd-α* signals (corresponding to the location of PGCs) later appeared close to the tail bud (TB) (**(C)** and close up inset, n = 4). At early pharyngula, *dnd-α* transcription marked the homed germ cells (black arrowheads) located as two distinctive lobes at the genital ridge (**(E)**, n = 7). While the *dnd-β* was first detected at the anterior region of the elongating body (**(B)** and close up inset, n = 4). The *dnd-β* signal emerged as a crescent line at the putative head of gastrula (n = 3) but expanded in both sides of the neural tube (NeT) at early segmentation (**(D)** and close up inset, n = 6) and eventually marked the metencephalon (MtCe) and cerebellum (CeB) of early pharyngula (**(F)**, n = 8) with no expression in Mesencephalon (MsCe) and diencephalon (DiCe). The compass indicates the orientation of body axis where applicable (a, anterior; p, posterior; d, dorsal and; v, ventral). The black dashed lines indicate the location of embryonic shield (**A,B**) or body (**C,D**). The white dashed line displays the expression area of *dnd-β* in hindbrain. The scales represent 100 and 250 μm in (**A′–D′**) and (**A–F**), respectively.

mechanisms. Specifically, the second major wave of epigenetic reprogramming in mice triggers around E6.5 (at the onset of gastrula) where PGCs are liberated from methylation (Gao and Das, 2014). This is simultaneous with PGC extrusion from the epiblast, *i.e.,* their specification from soma, *en route* to the genital ridge (Lee et al., 2014). In zebrafish, the pattern of DNA methylome is not fully comparable with those of mice (Potok et al., 2013), however, germ cell specific markers (e.g., *piwi, dazl,* and *vasa*) undergo hypomethylation post-ZGA during the sphere stage (Seisenberger et al., 2012; Potok et al., 2013; Hill et al., 2018). The timing of these

two events is concurrent with the surge in expression of *dazl* and *piwi II* at gastrula in *G. holbrooki*, a likely consequence of demethylation wave in the germline. However, this needs verification.

Expression Profile of Germline Markers Imply Sex-Dimorphic Proliferation of PGCs

A transient female-biased expression of PGC markers in *G. holbrooki* is similar to those of zebrafish (Ye et al., 2019) where preferential PGC proliferation leads to female differentiation. In zebrafish, the timing of PGC proliferation is known to occur as
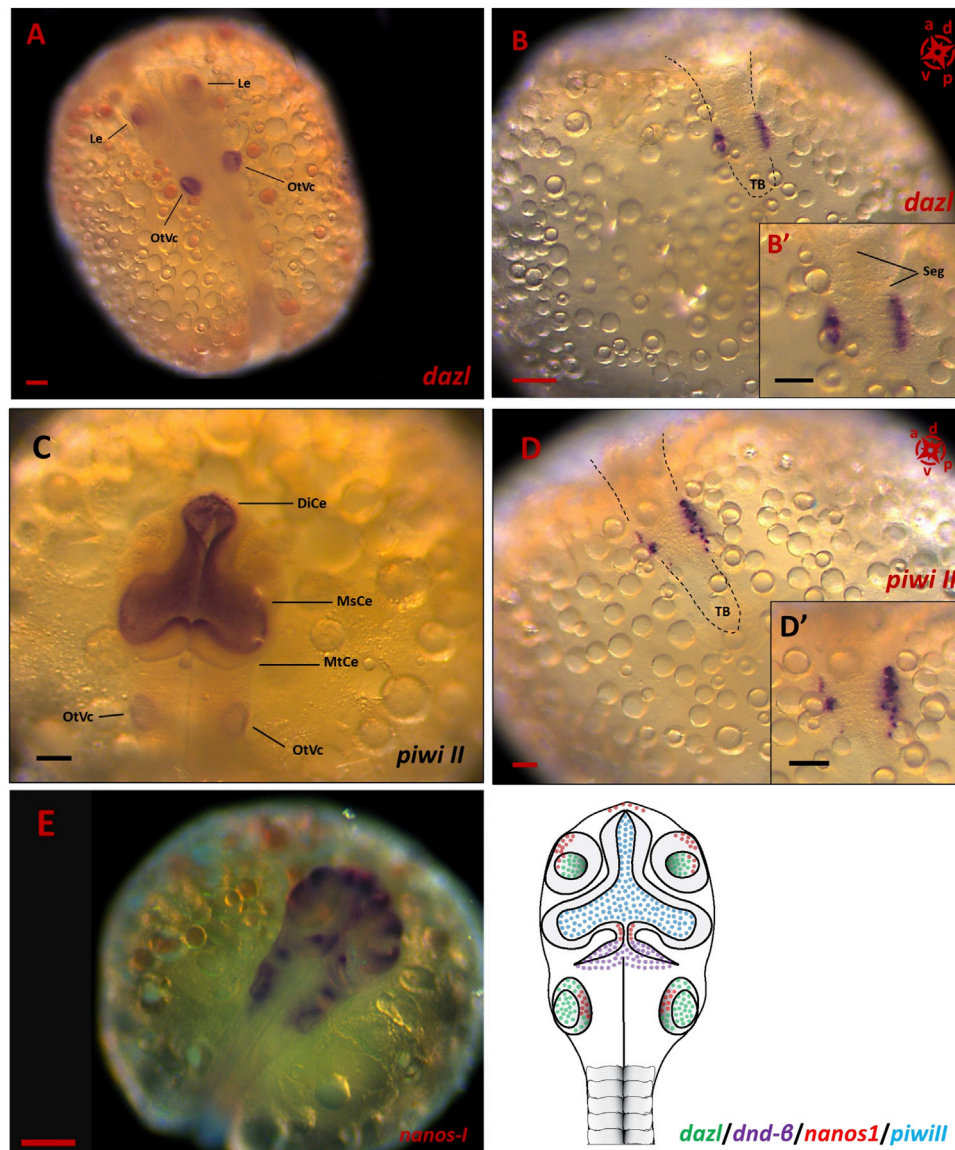
FIGURE 4 | The spatial expression of PGC markers in embryonic stages of *G. holbrooki*. WISH panels showing spatial expression of *dazl* **(A,B)**, *piwi ll* **(C,D)** and *nanos1* **(E)** during somitogenesis in *G. holbrooki*. The *dazl* expression (n = 5) was detected in otic vesicle (OtVc) and optic lens (Le), anteriorly **(A)** and PGC clusters posteriorly **(B)** and close up inset), in a closer proximity to tailbud (TB), right in both sides of segments (Seg). In slight contrast, the anterior expression of *piwi ll* (n = 7) was strongly detected in the region of developing brain predominantly in diencephalon (DiCe) and mesencephalon (MsCe) with a very weak expression in otic vesicles. Whereas the posterior expression of *piwi ll* was restricted to migrating PGCs (**(D)** and close up inset). The *nanos1* expression was exclusively detected in developing brain and otic vesicle of mid-somitogenesis embryos (n = 6). The compass indicates the orientation of developing embryos where applicable. The schematic **(F)** represents the simultaneous expression domains of PGC markers in CNS during somitogenesis. The black dashed lines indicate the location of embryonic body. The scale bars represent 100 μm.

early as gastrula (Feng et al., 2020) which begins between sphere and 50% epiboly (Wang et al., 2016). This parallels the evanescent upregulation of the markers in *G. holbrooki*, which likely corresponds to female-biased PGC proliferation.

PGC Migration Pattern Shares Features of Both Egg Laying Teleosts and Mouse

Consistent with the gene structure and content, the *vasa* and *dnd-α* expression in gambusia was restricted to the domains corresponding to PGCs. This was further supported by the restricted localisation of *vasa* transcript at the genital ridge of parturating embryos, where the newly formed gonad emerges. Although the molecular components and the machineries involved in PGC mobilisation are conserved among teleosts, the pattern of their migration varies between species (Saito et al., 2006). Typically, the early segregation of PGCs in teleosts relies on the localisation pattern of germ plasm, as the maternally inherited germ cell determinants (Bontems et al., 2009; Roovers et al., 2018). However, two types of germ plasm
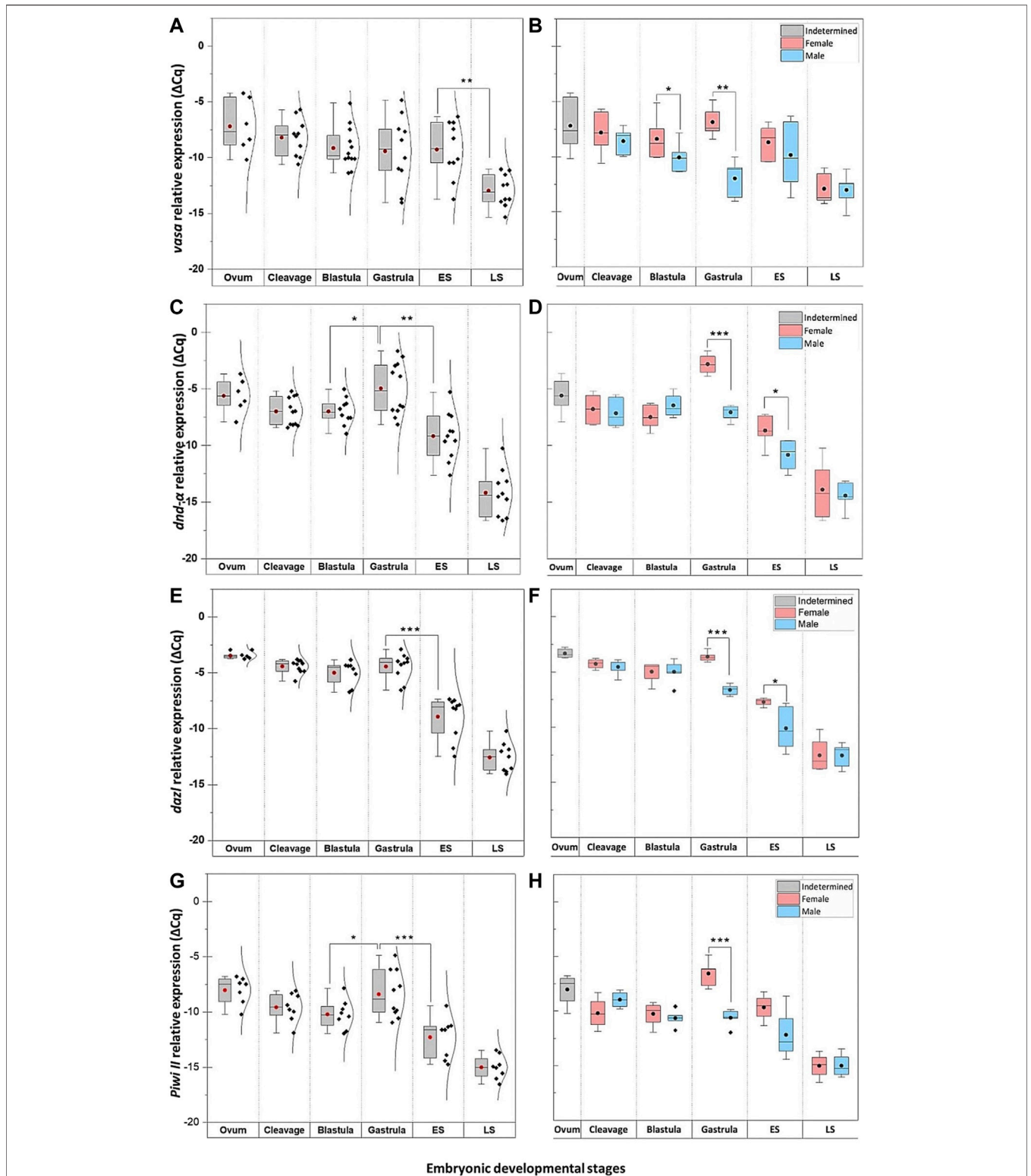
FIGURE 5 | The temporal expression of PGC markers at select embryonic stages of *G. holbrooki*. The pooled (left panel) and sex-segregated (right panel) quantitative expression of *vasa* **(A–B)**, *dnd-α* **(C–D)**), *dazl* **(E–F)**, and *piwiII* **(G–H)** in six embryonic developmental stages of *G. holbrooki*. ES, early somitogenesis; LS, late somitogenesis. The dots and the horizontal line within the bars indicate mean and median of the data presented within the groups. The normal distribution curves are given in the pooled expression plots. The asterisks show the level of significance between groups; Tuckey's HSD, * = 0.05, ** = 0.01, *** = 0.001.

FIGURE 6 | The temporal expression of *nanos1* and *dnd-β* at select embryonic stages of *G. holbrooki*. The panel representing quantitative expression of *nanos1* **(A)** and *dnd-β* **(B)** in six embryonic developmental stages of *G. holbrooki*. ES, early somitogenesis; LS, late somitogenesis. The dots and the line within the bars indicate mean and median of the data presented within the groups. The normal distribution curves are given in the global expression plots. The asterisks show the level of significance between the marked groups; Tuckey's HSD, * = 0.05, ** = 0.01, *** = 0.001.

arrangements have so far been described in early embryonic development of teleosts where (**Figure 7**); 1) germ plasm components aggregate compactly in cleavage furrows (Yabe et al., 2009) until the 16-cell stage, subsequently segregating into proliferating cells eventuating in four clusters of germ plasm-positive cells at the dome stage as in zebrafish (Raz, 2002), Atlantic cod, *Gadus morhua* (Presslauer et al., 2012), and olive flounder, *Paralichthys olivaceous* (Li et al., 2015) while in others, 2) the germ plasm signal is dissipated throughout the cell mass in early cell cycles with distinct germ plasm-positive cells first forming at the mid-gastrula stage, such as in medaka (Herpin et al., 2007). Although, the early cleavage stages could not be captured, the occurrence of four loosely aggregated clusters of *vasa*-positive cells at the periphery of blastodisc in *G. holbrooki* follows the former pattern (**Figure 7**).

The position of PGCs determines their migration start point which is defined in relation to cell collectivity and body patterning during blastula and gastrula stages, respectively (Raz, 2002). In zebrafish (Kimmel et al., 1995), medaka (Iwamatsu, 2004), and viviparous black rockfish (Zhou et al., 2020), prominent embryonic features (*e.g.,* sphere, yolk cell doming, multiple stages of epiboly) during blastula stage pose broad somatic environment for cell motility. While in poeciliids including *G. holbrooki* (Tavolga and Rugh, 1947; Tavolga, 1949; Mousavi and Patil, 2021), the blastodisc is extremely thin and flat and the growing cells sink inwards into the emerging yolk cavity. Therefore, cell patterning occurs in a relatively limited environment independent of yolk as a scaffold (dissimilar to zebrafish and medaka and similar to mice) where blastodisc does not grow over yolk cell to form dome. Indeed, the embryonic shield in *G. holbrooki* is relatively compact and at early gastrula swiftly begins to elongate and form embryonic body axis in the growing but restricted cavity on the yolk surface (Mousavi and

Patil, 2021). The dissimilarity in early embryonic body patterning (during blastula and gastrula) may affect the expression domain of chemokine signalling (*e.g.,* Cxcl12a-Cxcr4 interaction) as the key regulator of PGC migration in vertebrates. The formation of two clusters at early gastrula in gambusia, is comparable to the initial patterning of nascent germ cells in medaka (Saito et al., 2006; Kurokawa et al., 2007) where the PGCs are first found dispersed on both sides of the dorsal axis (Herpin et al., 2007).

During somitogenesis, PGC clusters in teleosts show two spatial patterns while migrating towards PGR. In one group including zebrafish (Weidinger et al., 1999), loach (Saito et al., 2006), and medaka (Herpin et al., 2007), the PGCs form two clusters positioned on either side, of the trunk and moving separately towards the genital ridge. In the second group including herring and floating goby (Saito et al., 2006), the two clusters converge towards the medial axis and transiently merge under the trunk during early somitogenesis. However, the merged PGC clusters, thereafter, split to form two distinct clusters in mid-somitogenesis. In *G. holbrooki*, PGC cluster formation and their mobility resembles the former pattern. In most teleosts, following the localisation of two clusters at body mid-line, the PGCs are localised anterior to the putative gonadal ridge (PGR), thereafter, homing posteriorly reaching the PGR (Saito et al., 2006; Herpin et al., 2007; Herpin et al., 2008). In contrast, the first appearance of these two PGC clusters posterior to the PGR and their subsequent anterior migration towards PGR, in *G. holbrooki*, appears a developmental novelty in teleosts. Interestingly, this resembles the pattern of PGC migration in mouse, where they are first specified in the posterior primitive streak, move to subjacent endoderm and migrate anteriorly towards gonadal ridge (Anderson et al., 2000; Saitou and Yamaji, 2012). During somitogenesis, the route of these PGC cluster migration in some teleosts, *e.g.,* medaka, loach and goldfish (Saito et al., 2006), are longer compared to those in zebrafish (Doitsidou et al., 2002), gobby

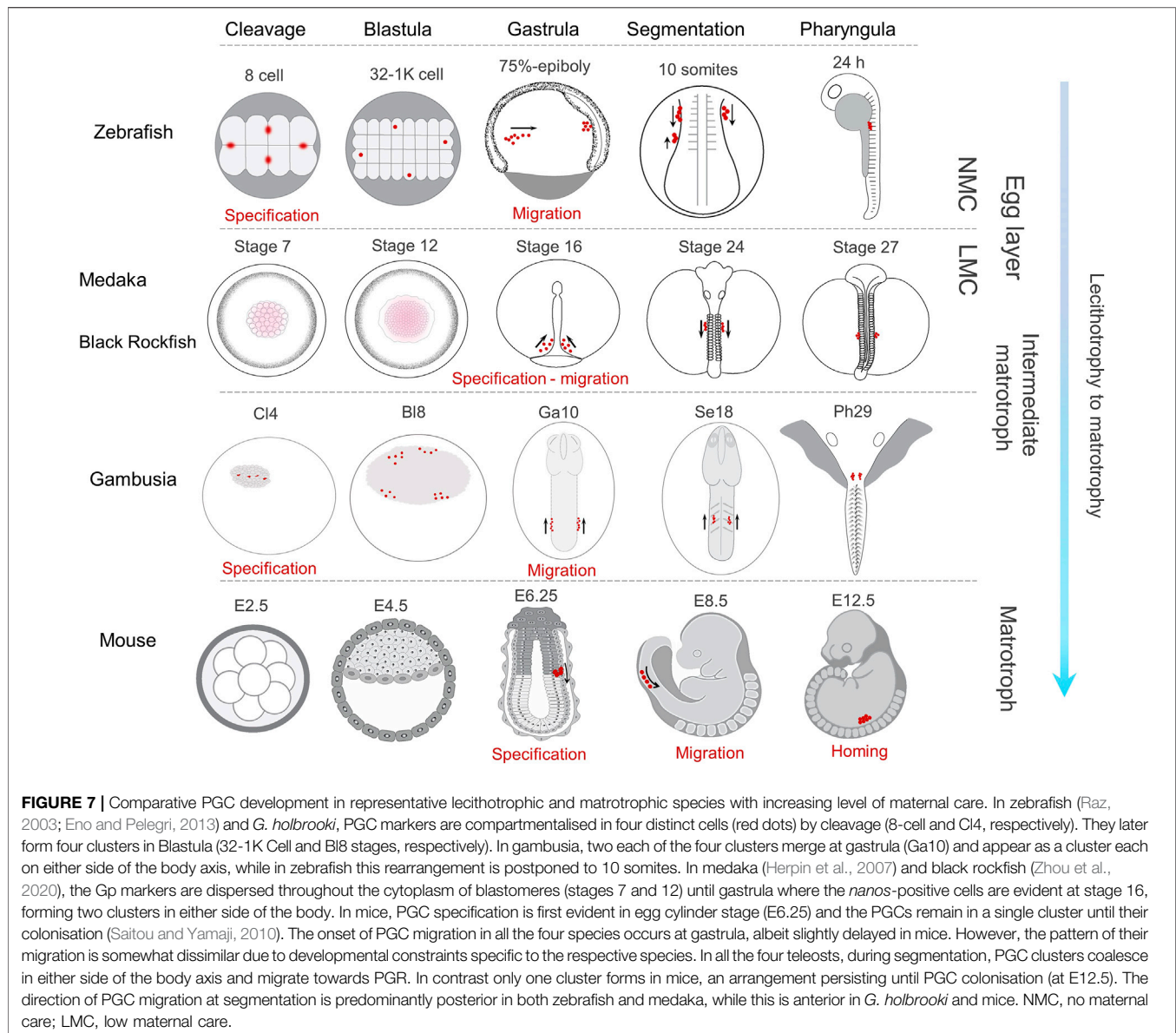**TABLE 1 |** Spatio-temporal expression of PGC-specific markers at select embryonic stages of *G. holbrooki*.

Genes	Spatio-temporal Expression		Ovum	Cleavage	Blastula	Gastrula	Early somitogenesis	Late somitogenesis	Figures
Vasa	Qualitative		—	- Tiny spots in blastomere (1A)	- Four clusters at the periphery of the blastodisc (1D)	- Two clusters at the margin of dome (1E and 1F)	- Posteriorly, at migrating PGC clusters (1G)	- PGR (1I)	**Figures 1, 2B**
	Quantitative	Between stages	−1.0 ± 1.0	−0.94 ± 0.75	−0.28 ± 1.06	−3.69 ± 0.91**	+0.14 ± 1.26		**Figure 5A**
		Between sex	—	0.78 ± 0.08 F	2.68 ± 1.02 F *	5.12 ± 1.01 F **	1.53 ± 2.03 F	0.11 ± 0.97 F	**Figure 5B**
dnd-α	Qualitative		—	- Tiny spots in blastomere	- Four clusters at the periphery of the blastodisc	- Two clusters at the margin of dome at vasa-positive cells (3A)	- Two PGC clusters close to the tail bud (3C)	- PGR (3E)	**Figures 1, 2B, 3**
	Quantitative	Between stages	−1.38 ± 0.66	−0.01 ± 0.52	+2.4 ± 0.81 *	−4.21 ± 0.92 ***	−5.2 ± 0.89 ***		**Figure 5C**
		Between sex	—	0.36 ± 0.73 F	1.70 ± 0.70 M	4.25 ± 0.42 F ***	2.15 ± 0.89 F *	0.52 ± 0.38 F	**Figure 5D**
dnd-β	Qualitative		—	—	—	- Anterior region of the elongating body (3B)	- Both sides of the neural tube (3D)	- Metencephalon and cerebellum (3F)	**Figures 2B, 3**
	Quantitative	Between stages	+6.71 ± 1.27 ***	−0.74 ± 0.61	−2.17 ± 0.61 *	−2.32 ± 0.76 **	−1.95 ± 0.78 *		**Figure 6A**
Dazl	Qualitative		—	- Tiny spots in blastomere	- Four clusters at the periphery of the blastodisc	- Two clusters at the margin of dome at vasa-positive cells	- Anteriorly, at optic lens and otic vesicles (4A). - Posteriorly, at PGC clusters (4B)	- Otic vesicles - Optic lens - PGR	**Figures 2B, 4**
	Quantitative	Between stages	−0.96 ± 0.28	−0.57 ± 0.39	+0.56 ± 0.53	−4.49 ± 0.70 ***	−3.64 ± 0.75 **		**Figure 5E**
		Between sex	—	0.28 ± 0.38 F	0.02 ± 0.72 M	3.01 ± 0.31 F ***	2.39 ± 0.94 F *	0.01 ± 0.93 M	**Figure 5F**
piwill	Qualitative		—	—	- Four clusters at the periphery of the blastodisc	—	- Anteriorly, at diencephalon and mesencephalon (4C). - Posteriorly, at PGC clusters (4D)	- diencephalon and mesencephalon, - PGR	**Figures 2B, 4**
	Quantitative	Between stages	−1.53 ± 0.62	−0.63 ± 0.65	+1.85 ± 0.86 *	−3.9 ± 0.95 F ***	−2.71 ± 0.75 **		**Figure 5G**
		Between sex	---	1.24 ± 0.83 M	0.40 ± 0.65 F	4.09 ± 0.67 F ***	2.5 ± 1.36 F	0.01 ± 0.80 F	**Figure 5H**
nanos1	Qualitative		—	—	—	- A single cluster at the anterior half	- Neural tube (4E) - Otic vesicles (4E)		**Figures 2B, 4**
	Quantitative	Between stages	+7.02 ± 1.27 ***	+2.16 ± 0.7 **	−2.89 ± 0.55 ***	−0.23 ± 0.61	−0.15 ± 0.45		**Figure 6B**

*Level of significance between groups (ΔΔCq, Tuckey's HSD): * = 0.05, ** = 0.01, *** = 0.001.*
The ΔΔCq between sexes were not significant for nanos1 *and* dnd-β *at any stage.*

and herring (Saito et al., 2006). In *G. holbrooki*, this migration from the posterior body cylinder to the PGR (*i.e.,* homing at 4–7 somites) appears even longer than medaka (10–12 somites) and loach (15–17 somites). This cellular remodelling (*i.e.,* migratory direction and relatively long migration path) may be attributed to the reproductive adaptation from lecithotrophy of egg layers to that of live-bearing. Conceivably, the organogenesis machinery directs the gonial stem cells to the far anterior part of the body in live-bearing fish to co-accommodate the complex anatomical novelty of a fused ovary and proto-uterus such as in *G. holbrooki*. This anterior location is perhaps reset more medially in mouse with the anatomical distinction of ovary and uterus. A comparative evaluation encompassing multiple poeciliids with increasing degree of matrotrophy will no doubt shed greater light on evolutionary relatedness of PGC development and lecitho-matrotrophy.

FIGURE 7 | Comparative PGC development in representative lecithotrophic and matrotrophic species with increasing level of maternal care. In zebrafish (Raz, 2003; Eno and Pelegri, 2013) and *G. holbrooki*, PGC markers are compartmentalised in four distinct cells (red dots) by cleavage (8-cell and CI4, respectively). They later form four clusters in Blastula (32-1K Cell and Bl8 stages, respectively). In gambusia, two each of the four clusters merge at gastrula (Ga10) and appear as a cluster each on either side of the body axis, while in zebrafish this rearrangement is postponed to 10 somites. In medaka (Herpin et al., 2007) and black rockfish (Zhou et al., 2020), the Gp markers are dispersed throughout the cytoplasm of blastomeres (stages 7 and 12) until gastrula where the *nanos*-positive cells are evident at stage 16, forming two clusters in either side of the body. In mice, PGC specification is first evident in egg cylinder stage (E6.25) and the PGCs remain in a single cluster until their colonisation (Saitou and Yamaji, 2010). The onset of PGC migration in all the four species occurs at gastrula, albeit slightly delayed in mice. However, the pattern of their migration is somewhat dissimilar due to developmental constraints specific to the respective species. In all the four teleosts, during segmentation, PGC clusters coalesce in either side of the body axis and migrate towards PGR. In contrast only one cluster forms in mice, an arrangement persisting until PGC colonisation (at E12.5). The direction of PGC migration at segmentation is predominantly posterior in both zebrafish and medaka, while this is anterior in *G. holbrooki* and mice. NMC, no maternal care; LMC, low maternal care.

Only *Vasa* and *Dnd-α* Exclusively Mark PGCs in *G. holbrooki*

The exclusive occurrence of *vasa* and *dnd-α* in PGCs of *G. holbrooki* is comparable to *vasa* (Yoon et al., 1997; Knaut et al., 2000; Su et al., 2014) and *dnd* (Hong et al., 2016; Wargelius et al., 2016) of other teleosts and those *vasa* (Tanaka et al., 2000) and *dnd-α* (Youngren et al., 2005) of mice. Inferred from its maternal inheritance and exclusive detection in migrating PGCs, *vasa* likely underpins PGC formation and function in *G. holbrooki*. This is consistent across taxa with maternally inherited mode of germline determination (Styhler et al., 1998; Kuznicki et al., 2000; Tanaka et al., 2000; Hickford et al., 2011). Functionally, the DEAD-box domain of VASA proteins underpin regulatory roles which restructure and remodel protein-coding RNAs to facilitate their translation (Linder, 2006; Sengoku et al., 2006). Thus, maternal *vasa* is likely to facilitate

the translation of Gp markers (predominantly stored in RNA form) in early zygotes of gambusia, as also occurs in lecithotrophic teleosts such as zebrafish (Knaut et al., 2002).

The abundant expression of maternal *dnd-α* in ova is likely associated with its essential role for specification and maintenance of PGCs in teleosts (Liu and Collodi, 2010; Hong et al., 2016). However, its established role as an anchor for maternal RNAs in unfertilised eggs and polymerization of cortical microtubule arrays has been demonstrated in *Xenopus* (Mei et al., 2013) needs verification in teleost. The subsequent occurrence of *dnd* in the embryonic and postnatal germline of *G. holbrooki* is consistent with those reported for other vertebrates (Youngren et al., 2005; Aramaki et al., 2007) including teleosts (Su et al., 2014; Duan et al., 2015; Wargelius et al., 2016) maintaining germline identity by protecting transcripts from miRNA-mediated decay (Ketting, 2007; Goudarzi et al., 2013),

facilitating translation of essential germ plasm components for PGC development (Aguero et al., 2017), preventing PGCs from soma differentiation (Weidinger et al., 2003; Gross-Thebing et al., 2017) and titrating the abundant mRNA through transcription silencing (Nousch et al., 2013; Yamaji et al., 2017). Taken together, the exclusive expression of *dnd-α* in gambusia germ cells encoding the essential regulatory domains suggests a conserved role for it in germline maintenance in this species and likely in other poeciliids.

Somatic Expression of Germline Markers May Confer Their Stemness

The non-germ cell-specific expression of *dazl*, *piwiII*, and *dnd-β*, in *G. holbrooki* is in accordance with the broader expression domain of these markers in invertebrates and higher vertebrates. For example, *Piwi* in invertebrates is also expressed in soma. Hence, it's a suggested role beyond germline maintenance, assisting in somatic cell cycles (Ma et al., 2014), tissue regeneration and homeostasis (Palakodeti et al., 2008), adaptive immunity (Miesen et al., 2015) and sex determination (Kiuchi et al., 2014). Also, the expression domain of *piwi* in PGC and CNS of *G. holbrooki* is in agreement with those of zebrafish (Tan et al., 2002), medaka (Li et al., 2012), and mammals (Kim, 2019).

This study, for the first time, reports the presence of an alternately spliced variant of *dnd* (*dnd-β*) in any teleost during its embryonic development. Interestingly, the somatic expression of *dnd-β* mostly resembles those reported (Bhattacharya et al., 2007) in pre-natal stages of mice. However, the content and expression domain of the variants in mice (Youngren et al., 2005) and gambusia are different. Specifically, in mice, the larger variant (*Dnd-α*) is detected in prenatal stages, both in PGCs and soma (*e.g.,* neuroectoderm, head mesenchyme, neural tube, and hindgut), while the shorter variant (*dnd-β*) takes over post-natal function in a germline-specific manner (Bhattacharya et al., 2008). Whereas in *G. holbrooki*, both variants are expressed in prenatal embryos albeit in different domains, with the shorter *dnd-β* retaining germ cell-specific expression as in mice.

More broadly, the study presents evidence for an expansion (*dnd-β*, *dazl*) in expression domains of germ cell-specific markers to soma in *G. holbrooki*. Indeed, these genes encode RBPs that facilitate cell differentiation and maintenance of early cell lineages in vertebrates (Guallar and Wang, 2014; Shigunov and Dallagiovanna, 2015) and invertebrates (Kerner et al., 2011) via silencing, protecting and/or enhancing translation. (Tsui et al., 2000), (Xu et al., 2013). Similarly, in *G. holbrooki*, the expression of germline-RBP genes in CNS represents an evolutionary diversification of function, likely associated with maintaining somatic stemness and its renewal (Isler, 2013; Tsuboi et al., 2018).

CONCLUSION

As a result of this study, our understanding of germ cell development in poeciliids has been markedly enhanced yielding insights shared with lecithotrophic teleosts as well as matrotrophic mammals. Specifically, the PGC-marker genes allowed the mode of PGC sequestration and position of germline to be determined. Remarkably, *G. holbrooki* retained preformation mode (*i.e.,* maternal inheritance) of specification (like teleosts) with a relatively early zygotic activation. Also, the early spatial pattern of PGCs resembled that of zebrafish, while the later migration pattern reminiscent of medaka and mouse, sharing the features of both lecithotrophy and matrotrophy. Consistent with this adaptation, the expression of teleostean germ cell markers in somatic cells confers stemness of the latter. Regardless, it is yet unclear if the shift in these molecular and cellular patterns led to evolution of the reproductive strategies or vice versa. In part, the adaptations in spatial patterns could be related to geometric restriction on developing embryo in matrotrophy compared to those of lecithotrophic teleosts, an aspect that needs verification. Showing the previously unsuspected conservation of elements specific to both lecithotrophic and matrotrophic organisms in *G. holbrooki*, lends itself as an excellent system to understand the evolutionary connectedness of germline development modes, reproductive adaptations and functional diversity of the germline markers. Like zebrafish, *G. holbrooki* is easy and relatively inexpensive to maintain, but display greater similarity to higher vertebrates, making it far more attractive system to study and understand mechanism of reproductive development and associated disease conditions of higher vertebrates. Also, a knowledge of PGC markers and functions is likely to provide pathways to develop species-specific solution for managing pest populations of this invasive species.

DATA AVAILABILITY STATEMENT

The datasets presented in this study can be found in online repositories. The names of the repository/repositories and accession number(s) can be found below: NCBI [accession: MZ542286-MZ542293].

ETHICS STATEMENT

The study was reviewed and approved by the University of Tasmania Animal Ethics Committee (Permit No. A12787).

AUTHOR CONTRIBUTIONS

KR: Conceptualization, investigation, methodology, data curation and analysis, validation, visualisation, resources, preparing original draft, review, and editing. JP: Conceptualization, methodology, validation, resources, supervision, funding acquisition, project administration, writing-review, and editing.

FUNDING

ACKNOWLEDGMENTS

SUPPLEMENTARY MATERIAL

The Supplementary Material for this article can be found online at: https://www.frontiersin.org/articles/10.3389/fcell.2022.793498/full#supplementary-material

REFERENCES

Aanes, H., Winata, C. L., Lin, C. H., Chen, J. P., Srinivasan, K. G., Lee, S. G. P., et al. (2011). Zebrafish mRNA Sequencing Deciphers Novelties in Transcriptome Dynamics during Maternal to Zygotic Transition. *Genome Res.* 21, 1328–1338. doi:10.1101/gr.116012.110

Abe, K. I., Yamamoto, R., Franke, V., Cao, M., Suzuki, Y., Suzuki, M. G., et al. (2015). The First Murine Zygotic Transcription Is Promiscuous and Uncoupled from Splicing and 3′ Processing. *EMBO J.* 34, 1523–1537. doi:10.15252/embj.201490648

Aguero, T., Jin, Z., Chorghade, S., Kalsotra, A., King, M. L., and Yang, J. (2017). Maternal Dead-End 1 Promotes Translation of Nanos1 by Binding the eIF3 Complex. *Development* 144, 3755–3765. doi:10.1242/dev.152611

Andersen, I. S., Reiner, A. H., Aanes, H., Aleström, P., and Collas, P. (2012). Developmental Features of DNA Methylation during Activation of the Embryonic Zebrafish Genome. *Genome Biol.* 13, R65. doi:10.1186/gb-2012-13-7-r65

Anderson, R., Copeland, T. K., Schöler, H., Heasman, J., and Wylie, C. (2000). The Onset of Germ Cell Migration in the Mouse Embryo. *Mech. Dev.* 91, 61–68. doi:10.1016/s0925-4773(99)00271-3

Aramaki, S., Sato, F., Kato, T., Soh, T., Kato, Y., and Hattori, M. A. (2007). Molecular Cloning and Expression of Dead End Homologue in Chicken Primordial Germ Cells. *Cell Tissue Res* 330, 45–52. doi:10.1007/s00441-007-0435-1

Atallah, J., and Lott, S. E. (2018). Evolution of Maternal and Zygotic mRNA Complements in the Early Drosophila Embryo. *Plos Genet.* 14, e1007838. doi:10.1371/journal.pgen.1007838

Ayres, R. M., Pettigrove, V. J., and Hoffmann, A. A. (2012). Genetic Structure and Diversity of Introduced Eastern Mosquitofish (Gambusia holbrooki) in South-Eastern Australia. *Mar. Freshw. Res.* 63. doi:10.1071/mf11279

Baroiller, J. F., D'Cotta, H., and Saillant, E. (2009). Environmental Effects on Fish Sex Determination and Differentiation. *Sex. Dev.* 3, 118–135. doi:10.1159/000223077

Bhattacharya, C., Aggarwal, S., Zhu, R., Kumar, M., Zhao, M., Meistrich, M. L., et al. (2007). The Mouse Dead-End Gene Isoform α Is Necessary for Germ Cell and Embryonic Viability. *Biochem. Biophys. Res. Commun.* 355, 194–199. doi:10.1016/j.bbrc.2007.01.138

Bhattacharya, C., Aggarwal, S., Kumar, M., Ali, A., and Matin, A. (2008). Mouse Apolipoprotein B Editing Complex 3 (APOBEC3) Is Expressed in Germ Cells and Interacts with Dead-End (DND1). *PLoS One* 3, e2315. doi:10.1371/journal.pone.0002315

Boldajipour, B., Mahabaleshwar, H., Kardash, E., Reichman-Fried, M., Blaser, H., Minina, S., et al. (2008). Control of Chemokine-Guided Cell Migration by Ligand Sequestration. *Cell* 132, 463–473. doi:10.1016/j.cell.2007.12.034

Bontems, F., Stein, A., Marlow, F., Lyautey, J., Gupta, T., Mullins, M. C., et al. (2009). Bucky ball Organizes Germ Plasm Assembly in Zebrafish. *Curr. Biol.* 19, 414–422. doi:10.1016/j.cub.2009.01.038

Braat, A. K., Van De Water, S., Korving, J., and Zivkovic, D. (2001). A Zebrafish Vasa Morphant Abolishes Vasa Protein but Does Not Affect the Establishment of the Germline. *Genesis* 30, 183–185. doi:10.1002/gene.1060

Chan, A. P., Kloc, M., Larabell, C. A., Legros, M., and Etkin, L. D. (2007). The Maternally Localized RNA Fatvg Is Required for Cortical Rotation and Germ Cell Formation. *Mech. Dev.* 124, 350–363. doi:10.1016/j.mod.2007.02.001

Chatfield, J., O'Reilly, M.-A., Bachvarova, R. F., Ferjentsik, Z., Redwood, C., Walmsley, M., et al. (2014). Stochastic Specification of Primordial Germ Cells from Mesoderm Precursors in Axolotl Embryos. *Development* 141, 2429–2440. doi:10.1242/dev.105346

Crother, B. I., White, M. E., and Johnson, A. D. (2016). Diversification and Germ-Line Determination Revisited: Linking Developmental Mechanism with Species Richness. *Front. Ecol. Evol.* 4, 26. doi:10.3389/fevo.2016.00026

Devlin, R. H., and Nagahama, Y. (2002). Sex Determination and Sex Differentiation in Fish: an Overview of Genetic, Physiological, and Environmental Influences. *Aquaculture* 208, 191–364. doi:10.1016/s0044-8486(02)00057-1

Doitsidou, M., Reichman-Fried, M., Stebler, J., Köprunner, M., Dörries, J., Meyer, D., et al. (2002). Guidance of Primordial Germ Cell Migration by the Chemokine SDF-1. *Cell* 111, 647–659. doi:10.1016/s0092-8674(02)01135-2

Donoughe, S., Nakamura, T., Ewen-Campen, B., Green, D. A., Henderson, L., and Extavour, C. G. (2014). BMP Signaling Is Required for the Generation of Primordial Germ Cells in an Insect. *Proc. Natl. Acad. Sci.* 111, 4133–4138. doi:10.1073/pnas.1400525111

Duan, J., Feng, G., Chang, P., Zhang, X., Zhou, Q., Zhong, X., et al. (2015). Germ Cell-specific Expression of *Dead End* (*Dnd*) in Rare Minnow (*Gobiocypris Rarus*). *Fish. Physiol. Biochem.* 41, 561–571. doi:10.1007/s10695-015-0029-x

Edgar, R. C. (2004). MUSCLE: Multiple Sequence Alignment with High Accuracy and High Throughput. *Nucleic Acids Res.* 32, 1792–1797. doi:10.1093/nar/gkh340

Eno, C., and Pelegri, F. (2013). Gradual Recruitment and Selective Clearing Generate Germ Plasm Aggregates in the Zebrafish Embryo. *Bioarchitecture* 3, 125–132. doi:10.4161/bioa.26538

Evans, T., Wade, C. M., Chapman, F. A., Johnson, A. D., and Loose, M. (2014). Acquisition of Germ Plasm Accelerates Vertebrate Evolution. *Science* 344, 200–203. doi:10.1126/science.1249325

Ewen-Campen, B., Schwager, E. E., and Extavour, C. G. M. (2010). The Molecular Machinery of Germ Line Specification. *Mol. Reprod. Dev.* 77, 3–18. doi:10.1002/mrd.21091

Extavour, C. G., and Akam, M. (2003). Mechanisms of Germ Cell Specification across the Metazoans: Epigenesis and Preformation. *Development* 130, 5869–5884. doi:10.1242/dev.00804

Feng, K., Cui, X., Song, Y., Tao, B., Chen, J., Wang, J., et al. (2020). Gnrh3 Regulates PGC Proliferation and Sex Differentiation in Developing Zebrafish. *Endocrinology* 161, bqz024. doi:10.1210/endocr/bqz024

Furness, A. I., Pollux, B. J. A., Meredith, R. W., Springer, M. S., and Reznick, D. N. (2019). How Conflict Shapes Evolution in Poeciliid Fishes. *Nat. Commun.* 10, 3335. doi:10.1038/s41467-019-11307-5

Furness, A. I., Avise, J. C., Pollux, B. J. A., Reynoso, Y., and Reznick, D. N. (2021). The Evolution of the Placenta in Poeciliid Fishes. *Curr. Biol.* 31, 2004–2011. doi:10.1016/j.cub.2021.02.008

Gao, F., and Das, S. K. (2014). Epigenetic Regulations through DNA Methylation and Hydroxymethylation: Clues for Early Pregnancy in Decidualization. *Biomol. Concepts* 5, 95–107. doi:10.1515/bmc-2013-0036

Gasparini, C., Pilastro, A., and Evans, J. P. (2011). Male Genital Morphology and its Influence on Female Mating Preferences and Paternity success in Guppies. *PLoS One* 6, e22329. doi:10.1371/journal.pone.0022329

Giraldez, A. J., Mishima, Y., Rihel, J., Grocock, R. J., Van Dongen, S., Inoue, K., et al. (2006). Zebrafish MiR-430 Promotes Deadenylation and Clearance of Maternal mRNAs. *Science* 312, 75–79. doi:10.1126/science.1122689

Goudarzi, M., Strate, I., Paksa, A., Lagendijk, A.-K., Bakkers, J., and Raz, E. (2013). On the Robustness of Germ Cell Migration and microRNA-Mediated Regulation of Chemokine Signaling. *Nat. Genet.* 45, 1264–1265. doi:10.1038/ng.2793

Grier, H. J., Burns, J. R., and Flores, J. A. (1981). Testis Structure in Three Species of Teleosts with Tubular Gonopodia. *Copeia* 1981, 797–801. doi:10.2307/1444180

Gross-Thebing, T., Yigit, S., Pfeiffer, J., Reichman-Fried, M., Bandemer, J., Ruckert, C., et al. (2017). The Vertebrate Protein Dead End Maintains Primordial Germ Cell Fate by Inhibiting Somatic Differentiation. *Dev. Cel* 43, 704–715. doi:10.1016/j.devcel.2017.11.019

Guallar, D., and Wang, J. (2014). RNA-binding Proteins in Pluripotency, Differentiation, and Reprogramming. *Front. Biol.* 9, 389–409. doi:10.1007/s11515-014-1326-y

Guzmán-Bárcenas, M. G., and Uribe, M. C. (2019). Superfetation in the Viviparous Fish *Heterandria Formosa* (Poeciliidae). *J. Morphol.* 280, 756–770. doi:10.1002/jmor.20982

Hansen, C. L., and Pelegri, F. (2021). Primordial Germ Cell Specification in Vertebrate Embryos: Phylogenetic Distribution and Conserved Molecular Features of Preformation and Induction. *Front. Cel Dev. Biol.* 9, 730332. doi:10.3389/fcell.2021.730332

Haraguchi, S., Tsuda, M., Kitajima, S., Sasaoka, Y., Nomura-Kitabayashid, A., Kurokawa, K., et al. (2003). *nanos1*: a Mouse Nanos Gene Expressed in the central Nervous System Is Dispensable for normal Development. *Mech. Dev.* 120, 721–731. doi:10.1016/s0925-4773(03)00043-1

Hartung, O., Forbes, M. M., and Marlow, F. L. (2014). Zebrafish Vasa Is Required for Germ-Cell Differentiation and Maintenance. *Mol. Reprod. Dev.* 81, 946–961. doi:10.1002/mrd.22414

Hellemans, J., Mortier, G., De Paepe, A., Speleman, F., and Vandesompele, J. (2007). qBase Relative Quantification Framework and Software for Management and Automated Analysis of Real-Time Quantitative PCR Data. *Genome Biol.* 8, R19. doi:10.1186/gb-2007-8-2-r19

Herpin, A., Rohr, S., Riedel, D., Kluever, N., Raz, E., and Schartl, M. (2007). Specification of Primordial Germ Cells in Medaka (Oryzias latipes). *BMC Dev. Biol.* 7, 3. doi:10.1186/1471-213x-7-3

Herpin, A., Fischer, P., Liedtke, D., Kluever, N., Neuner, C., Raz, E., et al. (2008). Sequential SDF1a and B-Induced Mobility Guides Medaka PGC Migration. *Dev. Biol.* 320, 319–327. doi:10.1016/j.ydbio.2008.03.030

Hickford, D. E., Frankenberg, S., Pask, A. J., Shaw, G., and Renfree, M. B. (2011). DDX4 (VASA) Is Conserved in Germ Cell Development in Marsupials and Monotremes. *Biol. Reprod.* 85, 733–743. doi:10.1095/biolreprod.111.091629

Hill, P. W. S., Leitch, H. G., Requena, C. E., Sun, Z., Amouroux, R., Roman-Trufero, M., et al. (2018). Epigenetic Reprogramming Enables the Transition from Primordial Germ Cell to Gonocyte. *Nature* 555, 392–396. doi:10.1038/nature25964

Hong, N., Li, M., Yuan, Y., Wang, T., Yi, M., Xu, H., et al. (2016). Dnd Is a Critical Specifier of Primordial Germ Cells in the Medaka Fish. *Stem Cel Rep.* 6, 411–421. doi:10.1016/j.stemcr.2016.01.002

Isler, K. (2013). Brain Size Evolution: How Fish Pay for Being Smart. *Curr. Biol.* 23, R63–R65. doi:10.1016/j.cub.2012.11.042

Iwamatsu, T. (2004). Stages of normal Development in the Medaka Oryzias latipes. *Mech. Dev.* 121, 605–618. doi:10.1016/j.mod.2004.03.012

Joseph, S. R., Pálfy, M., Hilbert, L., Kumar, M., Karschau, J., Zaburdaev, V., et al. (2017). Competition between Histone and Transcription Factor Binding Regulates the Onset of Transcription in Zebrafish Embryos. *Elife* 6, e23326. doi:10.7554/eLife.23326

Jukam, D., Shariati, S. A. M., and Skotheim, J. M. (2017). Zygotic Genome Activation in Vertebrates. *Dev. Cel* 42, 316–332. doi:10.1016/j.devcel.2017.07.026

Kaufman, O. H., and Marlow, F. L. (2016). Methods to Study Maternal Regulation of Germ Cell Specification in Zebrafish. *Methods Cel Biol.* 134, 1–32. doi:10.1016/bs.mcb.2016.02.001

Kerner, P., Degnan, S. M., Marchand, L., Degnan, B. M., and Vervoort, M. (2011). Evolution of RNA-Binding Proteins in Animals: Insights from Genome-wide Analysis in the Sponge Amphimedon Queenslandica. *Mol. Biol. Evol.* 28, 2289–2303. doi:10.1093/molbev/msr046

Ketting, R. F. (2007). A Dead End for microRNAs. *Cell* 131, 1226–1227. doi:10.1016/j.cell.2007.12.004

Kim, K. W. (2019). PIWI Proteins and piRNAs in the Nervous System. *Mol. Cell* 42, 828–835. doi:10.14348/molcells.2019.0241

Kimmel, C. B., Ballard, W. W., Kimmel, S. R., Ullmann, B., and Schilling, T. F. (1995). Stages of Embryonic Development of the Zebrafish. *Dev. Dyn.* 203, 253–310. doi:10.1002/aja.1002030302

Kiuchi, T., Koga, H., Kawamoto, M., Shoji, K., Sakai, H., Arai, Y., et al. (2014). A Single Female-specific piRNA Is the Primary Determiner of Sex in the Silkworm. *Nature* 509, 633–636. doi:10.1038/nature13315

Knaut, H., Pelegri, F., Bohmann, K., Schwarz, H., and Nüsslein-Volhard, C. (2000). Zebrafish Vasa RNA but Not its Protein Is a Component of the Germ Plasm and Segregates Asymmetrically before Germline Specification. *J. Cel Biol.* 149, 875–888. doi:10.1083/jcb.149.4.875

Knaut, H., Steinbeisser, H., Schwarz, H., and Nüsslein-Volhard, C. (2002). An Evolutionary Conserved Region in the Vasa 3′UTR Targets RNA Translation to the Germ Cells in the Zebrafish. *Curr. Biol.* 12, 454–466. doi:10.1016/s0960-9822(02)00723-6

Köprunner, M., Thisse, C., Thisse, B., and Raz, E. (2001). A Zebrafish Nanos-Related Gene Is Essential for the Development of Primordial Germ Cells. *Genes Dev.* 15, 2877–2885. doi:10.1101/gad.212401

Kurokawa, H., Saito, D., Nakamura, S., Katoh-Fukui, Y., Ohta, K., Baba, T., et al. (2007). Germ Cells Are Essential for Sexual Dimorphism in the Medaka Gonad. *Proc. Natl. Acad. Sci.* 104, 16958–16963. doi:10.1073/pnas.0609932104

Kuznicki, K. A., Smith, P. A., Leung-Chiu, W. M., Estevez, A. O., Scott, H. C., and Bennett, K. L. (2000). Combinatorial RNA Interference Indicates GLH-4 Can Compensate for GLH-1; These Two P Granule Components Are Critical for Fertility in *C. elegans*. *Development* 127, 2907–2916. doi:10.1242/dev.127.13.2907

Kwan, T. N., and Patil, J. G. (2019). Sex Biased Expression of Anti-mullerian Hormone (Amh) Gene in a Live Bearing Fish, Gambusia holbrooki: Evolutionary Implications and Potential Role in Sex Differentiation. *Comp. Biochem. Physiol. B Biochem. Mol. Biol.* 231, 59–66. doi:10.1016/j.cbpb.2019.02.004

Lai, F., Singh, A., and King, M. L. (2012). XenopusNanos1 Is Required to Prevent Endoderm Gene Expression and Apoptosis in Primordial Germ Cells. *Development* 139, 1476–1486. doi:10.1242/dev.079608

Lee, H. J., Hore, T. A., and Reik, W. (2014). Reprogramming the Methylome: Erasing Memory and Creating Diversity. *Cell Stem Cell* 14, 710–719. doi:10.1016/j.stem.2014.05.008

Li, M., Hong, N., Xu, H., Yi, M., Li, C., Gui, J., et al. (2009). Medaka Vasa Is Required for Migration but Not Survival of Primordial Germ Cells. *Mech. Dev.* 126, 366–381. doi:10.1016/j.mod.2009.02.004

Li, M., Hong, N., Gui, J., and Hong, Y. (2012). Medaka Piwi Is Essential for Primordial Germ Cell Migration. *Curr. Mol. Med.* 12, 1040–1049. doi:10.2174/156652412802480853

Li, M., Tan, X., Jiao, S., Wang, Q., Wu, Z., You, F., et al. (2015). A New Pattern of Primordial Germ Cell Migration in Olive Flounder (Paralichthys olivaceus) Identified Using Nanos3. *Dev. Genes Evol.* 225, 195–206. doi:10.1007/s00427-015-0503-6

Li, M., Zhu, F., Li, Z., Hong, N., and Hong, Y. (2016). Dazl Is a Critical Player for Primordial Germ Cell Formation in Medaka. *Sci. Rep.* 6, 28317. doi:10.1038/srep28317

Lindeman, R. E., and Pelegri, F. (2010). Vertebrate Maternal-Effect Genes: Insights into Fertilization, Early Cleavage Divisions, and Germ Cell Determinant Localization from Studies in the Zebrafish. *Mol. Reprod. Dev.* 77, 299–313. doi:10.1002/mrd.21128

Linder, P. (2006). Dead-box Proteins: a Family Affair-Active and Passive Players in RNP-Remodeling. *Nucleic Acids Res.* 34, 4168–4180. doi:10.1093/nar/gkl468

Liu, W., and Collodi, P. (2010). Zebrafish Dead End Possesses ATPase Activity that Is Required for Primordial Germ Cell Development. *FASEB J.* 24, 2641–2650. doi:10.1096/fj.09-148403

Liu, G., Wang, W., Hu, S., Wang, X., and Zhang, Y. (2018). Inherited DNA Methylation Primes the Establishment of Accessible Chromatin during Genome Activation. *Genome Res.* 28, 998–1007. doi:10.1101/gr.228833.117

Livak, K. J., and Schmittgen, T. D. (2001). Analysis of Relative Gene Expression Data Using Real-Time Quantitative PCR and the 2−ΔΔCT Method. *Methods* 25, 402–408. doi:10.1006/meth.2001.1262

Ma, X., Wang, S., Do, T., Song, X., Inaba, M., Nishimoto, Y., et al. (2014). Piwi Is Required in Multiple Cell Types to Control Germline Stem Cell Lineage

Development in the Drosophila Ovary. *PLoS One* 9, e90267. doi:10.1371/journal.pone.0090267

Matsuda, M. (2005). Sex Determination in the Teleost Medaka, *Oryzias latipes*. *Annu. Rev. Genet.* 39, 293–307. doi:10.1146/annurev.genet.39.110304.095800

Mei, W., Jin, Z., Lai, F., Schwend, T., Houston, D. W., King, M. L., et al. (2013). Maternal Dead-End1 Is Required for Vegetal Cortical Microtubule Assembly during *Xenopus* axis Specification. *Development* 140, 2334–2344. doi:10.1242/dev.094748

Miesen, P., Girardi, E., and van Rij, R. P. (2015). Distinct Sets of PIWI Proteins Produce Arbovirus and Transposon-Derived piRNAs inAedes Aegyptimosquito Cells. *Nucleic Acids Res.* 43, 6545–6556. doi:10.1093/nar/gkv590

Morrison, K. R., Ngo, V., Cardullo, R. A., and Reznick, D. N. (2017). How Fish Eggs Are Preadapted for the Evolution of Matrotrophy. *Proc. Biol. Sci.* 284, 20171342. doi:10.1098/rspb.2017.1342

Mousavi, S. E., and Patil, J. G. (2021). Stages of Embryonic Development in the Live-Bearing Fish, *Gambusia holbrooki*. *Dev. Dyn.*, 1–34. doi:10.1002/dvdy.388

Murata, K., Kinoshita, M., Naruse, K., Tanaka, M., and Kamei, Y. (2020). "Reproductive Behavior of Wild Japanese Medaka," in *Medaka: Biology, Management, and Experimental Protocols*. Editors K. Murata, M. Kinoshita, K. Naruse, M. Tanaka, and Y. Kamei. First ed. (New York; John Wiley & Sons).

Nagasawa, K., Fernandes, J. M. O., Yoshizaki, G., Miwa, M., and Babiak, I. (2013). Identification and Migration of Primordial Germ Cells in Atlantic salmon, Salmo salar : Characterization of Vasa , Dead End , and Lymphocyte Antigen 75 Genes. *Mol. Reprod. Dev.* 80, 118–131. doi:10.1002/mrd.22142

Norazmi-Lokman, N. H., Purser, G. J., and Patil, J. G. (2016). Gravid Spot Predicts Developmental Progress and Reproductive Output in a Livebearing Fish, *Gambusia holbrooki*. *PLoS One* 11, e0147711. doi:10.1371/journal.pone.0147711

Norazmi-Lokman, N. H., Purser, G. J., and Patil, J. G. (2021). Efficacy of Estradiol in Feminising the Eastern Mosquitofish, Gambusia holbrooki: advance towards Developing a Genetic Control Option. *Mar. Freshw. Res.* 72, 1657–1666. doi:10.1071/mf21104

Nousch, M., Techritz, N., Hampel, D., Millonigg, S., and Eckmann, C. R. (2013). The Ccr4-Not Deadenylase Complex Constitutes the Main Poly(A) Removal Activity in *C. elegans*. *J. Cel Sci.* 126, 4274–4285. doi:10.1242/jcs.132936

Olivera-Tlahuel, C., Moreno-Mendoza, N. A., Villagrán-Santa Cruz, M., and Zúñiga-Vega, J. J. (2018). Placental Structures and Their Association with Matrotrophy and Superfetation in Poeciliid Fishes. *Acta Zool.*100, 167–181. doi:10.1111/azo.12244

Paksa, A., and Raz, E. (2015). Zebrafish Germ Cells: Motility and Guided Migration. *Curr. Opin. Cel Biol.* 36, 80–85. doi:10.1016/j.ceb.2015.07.007

Pala, M. (1970). The Embryonic History of the Primordial Germ Cells inGambusia Holbrookii(Grd). *Bolletino di Zool.* 37, 49–62. doi:10.1080/11250007009440098

Palakodeti, D., Smielewska, M., Lu, Y.-C., Yeo, G. W., and Graveley, B. R. (2008). The PIWI Proteins SMEDWI-2 and SMEDWI-3 Are Required for Stem Cell Function and piRNA Expression in Planarians. *RNA* 14, 1174–1186. doi:10.1261/rna.1085008

Panina, Y., Germond, A., Masui, S., and Watanabe, T. M. (2018). Validation of Common Housekeeping Genes as Reference for qPCR Gene Expression Analysis during iPS Reprogramming Process. *Sci. Rep.* 8, 8716. doi:10.1038/s41598-018-26707-8

Patil, J. G., Norazmi-Lokman, N. H., and Kwan, T. N. (2020). Reproductive Viability of Paradoxically Masculinised *Gambusia holbrooki* Generated Following Diethylstilbestrol (DES) Treatment. *Comp. Biochem. Physiol. B Biochem. Mol. Biol.* 248-249, 110468–110477. doi:10.1016/j.cbpb.2020.110468

Patil, J. G. (2012). *An Adaptive Genetic Management Plan for Eradication of* Gambusia holbrooki *from Tasmania Australia*. New Norfolk, Tasmania: Inland Fisheries Service.

Pelegri, F. (2003). Maternal Factors in Zebrafish Development. *Dev. Dyn.* 228, 535–554. doi:10.1002/dvdy.10390

Pollux, B. J. A., Meredith, R. W., Springer, M. S., Garland, T., and Reznick, D. N. (2014). The Evolution of the Placenta Drives a Shift in Sexual Selection in Livebearing Fish. *Nature* 513, 233–236. doi:10.1038/nature13451

Potok, M. E., Nix, D. A., Parnell, T. J., and Cairns, B. R. (2013). Reprogramming the Maternal Zebrafish Genome after Fertilization to Match the Paternal Methylation Pattern. *Cell* 153, 759–772. doi:10.1016/j.cell.2013.04.030

Presslauer, C., Nagasawa, K., Fernandes, J. M. O., and Babiak, I. (2012). Expression of *Vasa* and *Nanos3* during Primordial Germ Cell Formation and Migration in Atlantic Cod (*Gadus morhua* L.). *Theriogenology* 78, 1262–1277. doi:10.1016/j.theriogenology.2012.05.022

Raz, E. (2002). Primordial Germ Cell Development in Zebrafish. *Semin. Cel Dev. Biol.* 13, 489–495. doi:10.1016/s1084952102001027

Raz, E. (2003). Primordial Germ-Cell Development: the Zebrafish Perspective. *Nat. Rev. Genet.* 4, 690–700. doi:10.1038/nrg1154

Richardson, B. E., and Lehmann, R. (2010). Mechanisms Guiding Primordial Germ Cell Migration: Strategies from Different Organisms. *Nat. Rev. Mol. Cel Biol.* 11, 37–49. doi:10.1038/nrm2815

Roberts, R. M., Green, J. A., and Schulz, L. C. (2016). The Evolution of the Placenta. *Reproduction* 152, R179–R189. doi:10.1530/rep-16-0325

Rongo, C., and Lehmann, R. (1996). Regulated Synthesis, Transport and Assembly of the *Drosophila* Germ Plasm. *Trends Genet.* 12, 102–109. doi:10.1016/0168-9525(96)81421-1

Roovers, E. F., Kaaij, L. J. T., Redl, S., Bronkhorst, A. W., Wiebrands, K., De Jesus Domingues, A. M., et al. (2018). Tdrd6a Regulates the Aggregation of Buc into Functional Subcellular Compartments that Drive Germ Cell Specification. *Dev. Cel* 46, 285–301. doi:10.1016/j.devcel.2018.07.009

Rothe, M., Pehl, M., Taubert, H., and Jäckle, H. (1992). Loss of Gene Function through Rapid Mitotic Cycles in the Drosophila Embryo. *Nature* 359, 156–159. doi:10.1038/359156a0

Ruijter, J. M., Ramakers, C., Hoogaars, W. M. H., Karlen, Y., Bakker, O., Van Den Hoff, M. J. B., et al. (2009). Amplification Efficiency: Linking Baseline and Bias in the Analysis of Quantitative PCR Data. *Nucleic Acids Res.* 37, e45. doi:10.1093/nar/gkp045

Ruzov, A., Dunican, D. S., Prokhortchouk, A., Pennings, S., Stancheva, I., Prokhortchouk, E., et al. (2004). Kaiso Is a Genome-wide Repressor of Transcription that Is Essential for Amphibian Development. *Development* 131, 6185–6194. doi:10.1242/dev.01549

Saito, T., Fujimoto, T., Maegawa, S., Inoue, K., Tanaka, M., Arai, K., et al. (2006). Visualization of Primordial Germ Cells *In Vivo* Using GFP-Nos1 3'UTR mRNA. *Int. J. Dev. Biol.* 50, 691–699. doi:10.1387/ijdb.062143ts

Saitou, M., and Yamaji, M. (2010). Germ Cell Specification in Mice: Signaling, Transcription Regulation, and Epigenetic Consequences. *Reproduction* 139, 931–942. doi:10.1530/rep-10-0043

Saitou, M., and Yamaji, M. (2012). Primordial Germ Cells in Mice. *Cold Spring Harb Perspect. Biol.* 4, a008375. doi:10.1101/cshperspect.a008375

Saitou, M., Kagiwada, S., and Kurimoto, K. (2012). Epigenetic Reprogramming in Mouse Pre-implantation Development and Primordial Germ Cells. *Development* 139, 15–31. doi:10.1242/dev.050849

Sakurai, T., Iguchi, T., Moriwaki, K., and Noguchi, M. (1995). The *Ter* Mutation First Causes Primordial Germ Cell Deficiency in *Ter/ter* Mouse Embryos at 8 Days of Gestation. *Dev. Growth Differ.* 37, 293–302. doi:10.1046/j.1440-169x.1995.t01-2-00007.x

Santos, A. C., and Lehmann, R. (2004). Germ Cell Specification and Migration in *Drosophila* and beyond. *Curr. Biol.* 14, R578–R589. doi:10.1016/j.cub.2004.07.018

Seisenberger, S., Andrews, S., Krueger, F., Arand, J., Walter, J., Santos, F., et al. (2012). The Dynamics of Genome-wide DNA Methylation Reprogramming in Mouse Primordial Germ Cells. *Mol. Cel* 48, 849–862. doi:10.1016/j.molcel.2012.11.001

Sengoku, T., Nureki, O., Nakamura, A., Kobayashi, S., and Yokoyama, S. (2006). Structural Basis for RNA Unwinding by the DEAD-Box Protein Drosophila Vasa. *Cell* 125, 287–300. doi:10.1016/j.cell.2006.01.054

Shigunov, P., and Dallagiovanna, B. (2015). Stem Cell Ribonomics: RNA-Binding Proteins and Gene Networks in Stem Cell Differentiation. *Front. Mol. Biosci.* 2, 74. doi:10.3389/fmolb.2015.00074

Smith, Z. D., and Meissner, A. (2013). DNA Methylation: Roles in Mammalian Development. *Nat. Rev. Genet.* 14, 204–220. doi:10.1038/nrg3354

Styhler, S., Nakamura, A., Swan, A., Suter, B., and Lasko, P. (1998). Vasa Is Required for GURKEN Accumulation in the Oocyte, and Is Involved in Oocyte Differentiation and Germline Cyst Development. *Development* 125, 1569–1578. doi:10.1242/dev.125.9.1569

Su, B., Peatman, E., Shang, M., Thresher, R., Grewe, P., Patil, J., et al. (2014). Expression and Knockdown of Primordial Germ Cell Genes, *Vasa, Nanos* and *Dead End* in Common Carp (*Cyprinus carpio*) Embryos for Transgenic

Sterilization and Reduced Sexual Maturity. *Aquaculture* 420-421, S72–S84. doi:10.1016/j.aquaculture.2013.07.008

Taguchi, A., Watanabe, K., and Orii, H. (2014). Intracellular Localizations of the Dead End Protein in Xenopus Primordial Germ Cells. *Int. J. Dev. Biol.* 58, 793–798. doi:10.1387/ijdb.140308ho

Tan, C.-H., Lee, T.-C., Weeraratne, S. D., Korzh, V., Lim, T.-M., and Gong, Z. (2002). *Ziwi*, the Zebrafish Homologue of the *Drosophila Piwi*: Co-localization with *Vasa* at the Embryonic Genital ridge and Gonad-specific Expression in the Adults. *Mech. Dev.* 119, S221–S224. doi:10.1016/s0925-4773(03)00120-5

Tanaka, S. S., Toyooka, Y., Akasu, R., Katoh-Fukui, Y., Nakahara, Y., Suzuki, R., et al. (2000). The Mouse Homolog of *Drosophila* Vasa Is Required for the Development of Male Germ Cells. *Genes Dev.* 14, 841–853. doi:10.1101/gad.14.7.841

Tavolga, W. N., and Rugh, R. (1947). Development of the Platyfish, *Platypoecilus Maculatus*. *Zool. Sci. Contrib. N. Y Zool. Soc.* 32, 1–15. doi:10.5962/p.206634

Tavolga, W. N. (1949). Embryonic Development of the Platyfish (*Platypoecilus*), the Swordtail (*Xiphophorus*), and Their Hybrids. *Bull. AMNH* 94, 165–229.

Thisse, C., and Thisse, B. (2008). High-resolution *In Situ* Hybridization to Whole-Mount Zebrafish Embryos. *Nat. Protoc.* 3, 59–69. doi:10.1038/nprot.2007.514

Toyooka, Y., Tsunekawa, N., TakahashiMATSUI, Y., Matsui, Y., Satoh, M., and Noce, T. (2000). Expression and Intracellular Localization of Mouse Vasa-homologue Protein during Germ Cell Development. *Mech. Dev.* 93, 139–149. doi:10.1016/s0925-4773(00)00283-5

Tsuboi, M., Van Der Bijl, W., Kopperud, B. T., Erritzøe, J., Voje, K. L., Kotrschal, A., et al. (2018). Breakdown of Brain-Body Allometry and the Encephalization of Birds and Mammals. *Nat. Ecol. Evol.* 2, 1492–1500. doi:10.1038/s41559-018-0632-1

Tsui, S., Dai, T., Warren, S. T., Salido, E. C., and Yen, P. H. (2000). Association of the Mouse Infertility Factor DAZL1 with Actively Translating Polyribosomes. *Biol. Reprod.* 62, 1655–1660. doi:10.1095/biolreprod62.6.1655

Tu, Q., Cameron, R. A., and Davidson, E. H. (2014). Quantitative Developmental Transcriptomes of the Sea Urchin *Strongylocentrotus purpuratus*. *Dev. Biol.* 385, 160–167. doi:10.1016/j.ydbio.2013.11.019

Untergasser, A., Cutcutache, I., Koressaar, T., Ye, J., Faircloth, B. C., Remm, M., et al. (2012). Primer3-new Capabilities and Interfaces. *Nucleic Acids Res.* 40, e115. doi:10.1093/nar/gks596

Vandesompele, J., De Preter, K., Pattyn, F., Poppe, B., Van Roy, N., De Paepe, A., et al. (2002). Accurate Normalization of Real-Time Quantitative RT-PCR Data by Geometric Averaging of Multiple Internal Control Genes. *Genome Biol.* 3, RESEARCH0034. doi:10.1186/gb-2002-3-7-research0034

Walvig, F. (1963). "The Gonads and the Formation of the Sexual Cells," in *The Biology Of Myxine*. Editors A. Brodal and R. Fange (Norway: Oslo Universitetsforlaget).

Wang, J. Q., and Cao, W. G. (2016). Key Signaling Events for Committing Mouse Pluripotent Stem Cells to the Germline Fate. *Biol. Reprod.* 94, 24. doi:10.1095/biolreprod.115.135095

Wang, H., Liu, Y., Ye, D., Li, J., Liu, J., and Deng, F. (2016). Knockdown of Zebrafish Nanog Increases Primordial Germ Cells during Early Embryonic Development. *Develop. Growth Differ.* 58, 355–366. doi:10.1111/dgd.12279

Wargelius, A., Leininger, S., Skaftnesmo, K. O., Kleppe, L., Andersson, E., Taranger, G. L., et al. (2016). Dnd Knockout Ablates Germ Cells and Demonstrates Germ Cell Independent Sex Differentiation in Atlantic salmon. *Sci. Rep.* 6, 21284. doi:10.1038/srep21284

Weidinger, G., Wolke, U., Köprunner, M., Klinger, M., and Raz, E. (1999). Identification of Tissues and Patterning Events Required for Distinct Steps in Early Migration of Zebrafish Primordial Germ Cells. *Development* 126, 5295–5307. doi:10.1242/dev.126.23.5295

Weidinger, G., Stebler, J., Slanchev, K., Dumstrei, K., Wise, C., Lovell-Badge, R., et al. (2003). Dead End, a Novel Vertebrate Germ Plasm Component, Is Required for Zebrafish Primordial Germ Cell Migration and Survival. *Curr. Biol.* 13, 1429–1434. doi:10.1016/s0960-9822(03)00537-2

Whittle, C. A., and Extavour, C. G. (2017). Causes and Evolutionary Consequences of Primordial Germ-Cell Specification Mode in Metazoans. *Proc. Natl. Acad. Sci. USA* 114, 5784–5791. doi:10.1073/pnas.1610600114

Xu, X., Tan, X., Lin, Q., Schmidt, B., Engel, W., and Pantakani, D. V. K. (2013). Mouse Dazl and its Novel Splice Variant Functions in Translational Repression of Target mRNAs in Embryonic Stem Cells. *Biochim. Biophys. Acta Gene Regul. Mech.* 1829, 425–435. doi:10.1016/j.bbagrm.2012.12.010

Yabe, T., Ge, X., Lindeman, R., Nair, S., Runke, G., Mullins, M. C., et al. (2009). The Maternal-Effect Gene Cellular Island Encodes aurora B Kinase and Is Essential for Furrow Formation in the Early Zebrafish Embryo. *Plos Genet.* 5, e1000518. doi:10.1371/journal.pgen.1000518

Yabuta, Y., Kurimoto, K., Ohinata, Y., Seki, Y., and Saitou, M. (2006). Gene Expression Dynamics during Germline Specification in Mice Identified by Quantitative Single-Cell Gene Expression Profiling1. *Biol. Reprod.* 75, 705–716. doi:10.1095/biolreprod.106.053686

Yamaji, M., Jishage, M., Meyer, C., Suryawanshi, H., Der, E., Yamaji, M., et al. (2017). DND1 Maintains Germline Stem Cells via Recruitment of the CCR4-Not Complex to Target mRNAs. *Nature* 543, 568–572. doi:10.1038/nature21690

Ye, D., Zhu, L., Zhang, Q., Xiong, F., Wang, H., Wang, X., et al. (2019). Abundance of Early Embryonic Primordial Germ Cells Promotes Zebrafish Female Differentiation as Revealed by Lifetime Labeling of Germline. *Mar. Biotechnol. (NY)* 21 (2), 217–228. doi:10.1007/s10126-019-09874-1

Yoon, C., Kawakami, K., and Hopkins, N. (1997). Zebrafish *Vasa* Homologue RNA Is Localized to the Cleavage Planes of 2- and 4-Cell-Stage Embryos and Is Expressed in the Primordial Germ Cells. *Development* 124, 3157–3165. doi:10.1242/dev.124.16.3157

Youngren, K. K., Coveney, D., Peng, X., Bhattacharya, C., Schmidt, L. S., Nickerson, M. L., et al. (2005). The Ter Mutation in the Dead End Gene Causes Germ Cell Loss and Testicular Germ Cell Tumours. *Nature* 435, 360–364. doi:10.1038/nature03595

Zernicka-Goetz, M. (1998). Fertile Offspring Derived from Mammalian Eggs Lacking Either Animal or Vegetal Poles. *Development* 125, 4803–4808. doi:10.1242/dev.125.23.4803

Zhou, L., Wang, X., Du, S., Wang, Y., Zhao, H., Du, T., et al. (2020). Germline Specific Expression of a Vasa Homologue Gene in the Viviparous Fish Black Rockfish (Sebastes Schlegelii) and Functional Analysis of the Vasa 3′ Untranslated Region. *Front. Cel Dev. Biol.* 8, 575788. doi:10.3389/fcell.2020.575788

Zhu, T., Gui, L., Zhu, Y., Li, Y., and Li, M. (2018). Dnd Is Required for Primordial Germ Cell Specification in *Oryzias celebensis*. *Gene* 679, 36–43. doi:10.1016/j.gene.2018.08.068